GEOLOGICAL SURVEY OF CANADA
OPEN FILE 7852

Targeted Geoscience Initiative 4: Contributions to the Understanding of Precambrian Lode Gold Deposits and Implications for Exploration

A global database of gold deposits: quantification of multi-element ore signatures

Eric C. Grunsky[1], Benoît Dubé[2], Steffen Hagemann[3], and Carl W. Brauhart[3]

[1]Geological Survey of Canada, Ottawa, Ontario
[2]Geological Survey of Canada, Québec, Quebec
[3]University of Western Australia, Perth, West Australia, Australia

2015

© Her Majesty the Queen in Right of Canada, as represented by the Minister of Natural Resources Canada, 2015

This publication is available for free download through GEOSCAN (http://geoscan.nrcan.gc.ca/)

Recommended citation

Grunsky, E.C., Dubé, B., Hagemann, S., and Brauhart, C.W., 2015. A global database of gold deposits: quantification or multi-element ore signatures, *In:* Targeted Geoscience Initiative 4: Contributions to the Understanding of Precambrian Lode Gold Deposits and Implications for Exploration, (ed.) B. Dubé and P. Mercier-Langevin; Geological Survey of Canada, Open File 7852, p. 271–285.

Publications in this series have not been edited; they are released as submitted by the author.

Contribution to the Geological Survey of Canada's Targeted Geoscience Initiative 4 (TGI-4) Program (2010–2015)

TABLE OF CONTENTS

A global database of gold deposits: quantification of multi-element ore signatures

Eric C. Grunsky[1]*, Benoît Dubé[2], Steffen Hagemann[3], and Carl W. Brauhart[3]

[1]Geological Survey of Canada, 601 Booth Street, Ottawa, Ontario K1A 0E9
[2]Geological Survey of Canada, 490 rue de la Couronne, Québec, Quebec G1K 9A9
[3]Centre for Exploration Targeting, University of Western Australia, 35 Stirling Highway Crawley, Perth, Western Australia 6009, Australia
*Corresponding author's e-mail: Eric.Grunsky@NRCan-RNCan.gc.ca

ABSTRACT

A new approach to characterizing and classifying mineral deposits based on whole-rock geochemistry is currently being developed jointly by the mineral exploration industry, the University of Western Australia, and the Geological Survey of Canada.

Based on 24 elements (Fe, Co, Ni, Re, Pd, Pt, Cu, Ag, Au, Zn, Cd, In, Tl, Pb, Hg, As, Sb, Bi, Te, Mo, W, Sn, La, U), a centred log-ratio transformation is used for representative samples of mineral deposits. Success of this approach requires the use of rigorous analytical protocols that have also been established for this project.

A component of this project is focused on the development of a statistical classification approach to cataloguing ore deposit styles. Research done to date, shows that this methodology has successfully identified a wide range of mineral deposit types including porphyry, lode gold, PGE, skarn, sedimentary rock-hosted massive sulphides, volcanic-hosted massive sulphides and Mississippi-type lead-zinc deposits. This contribution focuses solely on gold deposits.

Geochemical data of unknown metallogenic affinities can be classified and existing classifications can be enhanced/re-defined. The results indicate that trends and differences of a spectrum of gold deposits can be successfully classified using statistical methodologies and metrics for expressing ore chemistry. In conjunction with geological knowledge, this database and associated methodologies will enhance the recognition and classification of a range of lode gold deposit types and could be useful in both greenfields and brownfields exploration programs.

INTRODUCTION

Ore Samples Normalized to Average Crustal Abundance (OSNACA) is part of a broad initiative to characterize ore deposit signatures in a unique way such that geochemical similarities and differences between mineral deposit types can be quantified and classified. The OSNACA international project is a new approach jointly developed by the mineral exploration industry, the Centre for Exploration Targeting, University of Western Australia, and the TGI-4 Lode Gold project to characterize and classify ore samples from various mineral deposit types based on whole rock geochemistry. A technique (Brauhart et al., 2015) has been developed that quantifies differences in multi-element signatures or ore-deposit chemistry and defines a "magmato-hydrothermal space". Twenty-four elements define the mathematical space where an ore geochemical signature is defined by its "enrichment vector". Every sample must be analysed for every element used in the calculations. The database that comprises these ore samples is part of a larger database being assembled and defined by the OSNACA project (Brauhart et al., 2015) Research is being conducted on the development of a suitable metric to study ore-deposit chemistry.

Numerous workers have suggested a continuum between different ore-deposit classes such as Mississippi Valley type (MVT) and sedimentary-hosted massive sulphide (SHMS) (e.g. Leach et al., 2005), volcanic-hosted massive sulphide (VHMS) and epithermal (e.g. Hannington et al., 1999), porphyry and high-sulphidation epithermal (Sillitoe, 1989), orogenic Au, Carlin Au, and epithermal (Nesbitt, 1988), and even a link between iron oxide-copper-gold (IOCG) deposits and mantle-related mineralization (Groves et al., 2010). The integration of the deposits into a metric space has been termed the "Magmato-Hydrothermal Space". The latter is presented as a new means to document and quantitatively describe both the range and statistical uniqueness of ore-deposit types and clans.

Grunsky, E.C., Dubé, B., Hagemann, S., and Brauhart, C.W., 2015. A global database of gold deposits: quantification or multi-element ore signatures, *In:* Targeted Geoscience Initiative 4: Contributions to the Understanding of Precambrian Lode Gold Deposits and Implications for Exploration, (ed.) B. Dubé and P. Mercier-Langevin; Geological Survey of Canada, Open File 7852, p. 271–285.

Although the broader goals of the OSNACA project are to incorporate all deposit types into a geochemical metric, this report is limited to four main types of gold deposits: Carlin (Car), epithermal, high-sulphidation epithermal (HSEpi), low-sulphidation epithermal (LSEpi), and orogenic greenstone-hosted (OGs) (Table 1). The OSNACA database also contains seven gold deposits that are "intrusion-related". This population was considered too small to be considered for a statistical evaluation of gold deposits and these data were not included in this study. Two methodologies described for the OSNACA project include (1) examining the ratios of ore-deposit chemistry against average crustal abundance; and (2) centred log-ratio transformations (Aitchison, 1986). This study examines the centred log-ratio (clr) metric for characterization and classification of gold deposits. Geochemical data are compositional in nature and thus to identify patterns and features of the data that are not related to the data closure problem, a centred log-ratio transform was employed (Aitchison, 1986). Data discovery methods, including principal component analysis (PCA) and multi-dimensional scaling (MDS), were applied to the transformed data to assist in characterizing the different deposit types. Finally, a classification methodology (linear discriminant analysis; LDA) was applied to test the uniqueness of the established deposit classifications.

The results presented here represent a global collection of gold deposit samples, which includes many samples from Canada as part of the Targeted Geoscience Initiative 4 (TGI-4) Lode Gold Project. The samples contributed to the project are listed in Table 1.

Analytical Methods

Ore deposit samples were obtained from world-wide sources according to the following prerequisites.

- Ore samples must be from a substantial body of mineralization that could be mined profitably through modern mining techniques;
- Samples must be devoid of weathering effects;
- Samples must be from different parts of the ore deposit, with "run of the mill" samples preferred to obscure and unusual samples of the deposit;
- A minimum of 500 g of sample is recommended, but samples as small as 200 g were also analyzed; and
- The ore deposit is located by longitude and latitude [datum: WGS84] coordinates.

Samples were prepared on a diamond saw to produce a reference sample and an assay subsample of (ideally) more than 250 g. Samples were cut across layering or any dominant vein direction so that the assay sample and reference sample are as similar as possible. The entire assay sample was crushed at Bureau-Veritas – Ultratrace in a steel jaw crusher and then milled in a tungsten-carbide mill with a barren quartz wash between each sample. Four analytical techniques were performed:

1. 50 g Pb-collection fire assay with ICP-MS finish;
2. 20 g aqua regia digest with ICP-MS finish;
3. 0.15 g "four-acid" digest with ICP-MS and ICP-OES finish; and
4. 0.25 g peroxide fusion digest with ICP-MS and ICP-OES finish.

The first three analytical techniques are tailored to the 24 elements used in this paper, but we recognize that the OSNACA database has many different potential uses and therefore it is desirable to also capture all of the major elements and a wide suite of trace elements. The analytical techniques listed above are ideal for analysing for many of these additional elements, but not all. For example, major elements would better be analyzed by XRF but the extra cost is not warranted for the entire OSNACA collection.

Samples were submitted in batches of 48 with an additional blank sample and assay standard. All data is available at http://www.cet.edu.au/OSNACA.

The amount of publicly available geochemical data for ore deposits is extensive, but analytical techniques, detection limits, and above all, assay suites, vary widely. The subset of publically available datasets containing analyses for all 24 ore and pathfinder elements used here, with appropriate detection limits, is extremely limited. In response to this gap in available data, researchers at the Centre for Exploration Targeting at the University of Western Australia created the OSNACA database, a publicly available online resource providing consistent high-quality data of ore-deposit samples from around the world (OSNACA, 2013).

RESULTS AND DATA ANALYSIS

The results presented here represent a global collection of 178 gold deposit samples from a total of 431 analyses that currently comprise the OSNACA database. The TGI-4 Lode Gold Project provided 18 samples, mainly from Canadian orogenic gold deposits (see Table 1).

In the application of statistical methods requiring estimates of the mean and other moments, sample populations with censored data (data reported at less than the lower limit of detection) are biased. This is due values of less than the lower limit of detection are all reported only as that value. In order to minimize this bias, a replacement methodology (EM algorithm), which has documented by Palarea-Albaladejo et al. (2008), was used to find suitable replacement values.

Table 1. Listing of the gold deposit chemistry used in this study. Geochemical data available from the Ore Samples Normalized to Average Crustal Abundance (OSNACA) website (http://www.cet.edu.au/OSNACA).

Sample	Deposit Name	CharCode	Country	State	Class	SubClass	WClass	Longitude	Latitude
700077	Betze-Post	BZP	USA	Nevada	Carlin Au	Carlin Au	Car	-116.376037	40.980021
700078	Betze-Post	BZP	USA	Nevada	Carlin Au	Carlin Au	Car	-116.376037	40.980021
700079	Gold Quarry	GQY	USA	Nevada	Carlin Au	Carlin Au	Car	-116.215976	40.782255
700080	Gold Quarry	GQY	USA	Nevada	Carlin Au	Carlin Au	Car	-116.215976	40.782255
700081	Rain	RAI	USA	Nevada	Carlin Au	Carlin Au	Car	-116.011442	40.613802
700107	Gold Quarry	GQY	USA	Nevada	Carlin Au	Carlin Au	Car	-116.215976	40.782255
700108	Gold Quarry	GQY	USA	Nevada	Carlin Au	Carlin Au	Car	-116.215976	40.782255
700109	Rain	RAI	USA	Nevada	Carlin Au	Carlin Au	Car	-116.011442	40.613802
700110	Rain	RAI	USA	Nevada	Carlin Au	Carlin Au	Car	-116.011442	40.613802
700111	Betze-Post	BZP	USA	Nevada	Carlin Au	Carlin Au	Car	-116.376037	40.980021
700112	Betze-Post	BZP	USA	Nevada	Carlin Au	Carlin Au	Car	-116.376037	40.980021
700138	Mount Olympus	MTO	Australia	WA	Carlin Au	Carlin Au	Car	117.900151	-23.432301
700139	Mount Olympus	MTO	Australia	WA	Carlin Au	Carlin Au	Car	117.900151	-23.432301
700140	Mount Olympus	MTO	Australia	WA	Carlin Au	Carlin Au	Car	117.900151	-23.432301
700141	Mount Olympus	MTO	Australia	WA	Carlin Au	Carlin Au	Car	117.900151	-23.432301
700142	Mount Olympus	MTO	Australia	WA	Carlin Au	Carlin Au	Car	117.900151	-23.432301
700143	Mount Olympus	MTO	Australia	WA	Carlin Au	Carlin Au	Car	117.900151	-23.432301
700144	Mount Olympus Peake	MTO	Australia	WA	Carlin Au	Carlin Au	Car	117.873183	-23.43358
700244	Florida Canyon	FLC	USA	Nevada	Carlin Au	Carlin Au	Car	-118.242	40.574
700245	Florida Canyon	FLC	USA	Nevada	Carlin Au	Carlin Au	Car	-118.242	40.574
700246	Twin Creeks	TWC	USA	Nevada	Carlin Au	Carlin Au	Car	-117.172802	41.245
700247	Gold Quarry	GQY	USA	Nevada	Carlin Au	Carlin Au	Car	-116.216	40.7823
700248	Gold Quarry	GQY	USA	Nevada	Carlin Au	Carlin Au	Car	-116.216	40.7823
700251	Gold Quarry	GQY	USA	Nevada	Carlin Au	Carlin Au	Car	-116.216	40.7823
700252	Betze-Post	BZP	USA	Nevada	Carlin Au	Carlin Au	Car	-116.376037	40.980021
700253	Betze-Post	BZP	USA	Nevada	Carlin Au	Carlin Au	Car	-116.376037	40.980021
700046	Equity	EQU	USA	Colorado	Epithermal	Low-Sulphidation Epithermal	LSEpi	-106.959618	37.939382
700047	Equity	EQU	USA	Colorado	Epithermal	Low-Sulphidation Epithermal	LSEpi	-106.959618	37.939382
700294	Lake Cowal	LCW	Australia	NSW	Epithermal	Low-Sulphidation Epithermal	LSEpi	147.404323	-33.639494
700295	Lake Cowal	LCW	Australia	NSW	Epithermal	Low-Sulphidation Epithermal	LSEpi	147.404168	-33.639397
700296	Lake Cowal	LCW	Australia	NSW	Epithermal	Low-Sulphidation Epithermal	LSEpi	147.404034	-33.639324
700297	Lake Cowal	LCW	Australia	NSW	Epithermal	Low-Sulphidation Epithermal	LSEpi	147.405683	-33.637445
700298	Lake Cowal	LCW	Australia	NSW	Epithermal	Low-Sulphidation Epithermal	LSEpi	147.405741	-33.637816
700357	Lake Cowal	LCW	Australia	NSW	Epithermal	Low-Sulphidation Epithermal	LSEpi	147.404544	-33.635096
700358	Lake Cowal	LCW	Australia	NSW	Epithermal	Low-Sulphidation Epithermal	LSEpi	147.404781	-33.635956
700359	Lake Cowal	LCW	Australia	NSW	Epithermal	Low-Sulphidation Epithermal	LSEpi	147.404802	-33.635052
700360	Lake Cowal	LCW	Australia	NSW	Epithermal	Low-Sulphidation Epithermal	LSEpi	147.404762	-33.635162
700361	Lake Cowal	LCW	Australia	NSW	Epithermal	Low-Sulphidation Epithermal	LSEpi	147.406022	-33.634852
700362	Lake Cowal	LCW	Australia	NSW	Epithermal	Low-Sulphidation Epithermal	LSEpi	147.406252	-33.634843
700363	Lake Cowal	LCW	Australia	NSW	Epithermal	Low-Sulphidation Epithermal	LSEpi	147.405539	-33.639371
700181	Lake Cowal	LCW	Australia	NSW	Epithermal	Low-Sulphidation Epithermal	LSEpi	147.408087	-33.638148
700182	Lake Cowal	LCW	Australia	NSW	Epithermal	Low-Sulphidation Epithermal	LSEpi	147.405551	-33.637239
700183	Lake Cowal	LCW	Australia	NSW	Epithermal	Low-Sulphidation Epithermal	LSEpi	147.405482	-33.637487
700184	Lake Cowal	LCW	Australia	NSW	Epithermal	Low-Sulphidation Epithermal	LSEpi	147.407125	-33.636367

Table 1 continued.

Sample	Deposit Name	CharCode	Country	State	Class	SubClass	WClass	Longitude	Latitude
700185	Lake Cowal	LCW	Australia	NSW	Epithermal	Low-Sulphidation Epithermal	LSEpi	147.407158	-33.636391
700186	Lake Cowal	LCW	Australia	NSW	Epithermal	Low-Sulphidation Epithermal	LSEpi	147.407137	-33.63636
700187	Lake Cowal	LCW	Australia	NSW	Epithermal	Low-Sulphidation Epithermal	LSEpi	147.40721	-33.636532
700188	Lake Cowal	LCW	Australia	NSW	Epithermal	Low-Sulphidation Epithermal	LSEpi	147.407241	-33.63657
700189	Lake Cowal	LCW	Australia	NSW	Epithermal	Low-Sulphidation Epithermal	LSEpi	147.407156	-33.63646
700163	Hishikari	HIS	Japan	Kagoshima	Epithermal	Epithermal Low-Sulphidation	HSEpi	130.696207	32.013132
700164	Hishikari	HIS	Japan	Kagoshima	Epithermal	Epithermal Low-Sulphidation	HSEpi	130.696207	32.013132
700059	Akeshi	AKH	Japan	Kagoshima	Epithermal	High-Sulphidation Epithermal	HSEpi	130.380279	31.309986
700060	Akeshi	AKH	Japan	Kagoshima	Epithermal	High-Sulphidation Epithermal	HSEpi	130.380279	31.309986
700061	Kasuga	KAS	Japan	Kagoshima	Epithermal	High-Sulphidation Epithermal	HSEpi	130.256945	31.270014
700062	Kasuga	KAS	Japan	Kagoshima	Epithermal	High-Sulphidation Epithermal	HSEpi	130.256945	31.270014
700063	Kasuga	KAS	Japan	Kagoshima	Epithermal	High-Sulphidation Epithermal	HSEpi	130.256945	31.270014
700064	Castle Mountain	CAM	USA	California	Epithermal	High-Sulphidation Epithermal	HSEpi	-115.100184	35.284472
700065	Castle Mountain	CAM	USA	California	Epithermal	High-Sulphidation Epithermal	HSEpi	-115.100184	35.284472
700066	Ohakuri	OHA	New Zealand	Waikato	Epithermal	High-Sulphidation Epithermal	HSEpi	176.086035	-38.404594
700067	Ohakuri	OHA	New Zealand	Waikato	Epithermal	High-Sulphidation Epithermal	HSEpi	176.086035	-38.404594
700068	Ohakuri	OHA	New Zealand	Waikato	Epithermal	High-Sulphidation Epithermal	HSEpi	176.086035	-38.404594
700069	Martha	MAR	New Zealand	Waikato	Epithermal	High-Sulphidation Epithermal	HSEpi	175.842267	-37.386383
700070	Martha	MAR	New Zealand	Waikato	Epithermal	High-Sulphidation Epithermal	HSEpi	175.842267	-37.386383
700441	Chelopech	CLP	Bulgaria		Epithermal	High-Sulphidation Epithermal	HSEpi	24.073247	42.695752
700462	Chesney	CSY	Australia	NSW	Epithermal	High-Sulphidation Epithermal	HSEpi	145.85	-31.52
700463	Chesney	CSY	Australia	NSW	Epithermal	High-Sulphidation Epithermal	HSEpi	145.85	-31.52
700464	Chesney	CSY	Australia	NSW	Epithermal	High-Sulphidation Epithermal	HSEpi	145.85	-31.52
700087	Brewer	BRW	USA	Alaska	Epithermal	High-Sulphidation Epithermal	HSEpi	-80.417197	34.653015
700093	Haile	HAI	USA	South Carolina	Epithermal	High-Sulphidation Epithermal	HSEpi	-80.533613	34.580796
700094	Haile	HAI	USA	South Carolina	Epithermal	High-Sulphidation Epithermal	HSEpi	-80.533613	34.580796
700442	Rosia Montana	RSM	Romania		Epithermal	High-Sulphidation Epithermal	HSEpi	23.122895	46.298785
700443	Rosia Montana	RSM	Romania		Epithermal	High-Sulphidation Epithermal	HSEpi	23.122895	46.298785
700090	Fort Knox	FTK	USA	Alaska	Orogenic - Intrusion-Related Au	High-Sulphidation Epithermal	IR	-147.360601	64.992228
700091	Fort Knox	FTK	USA	Alaska	Orogenic - Intrusion-Related Au	Intrusion-Related Au	IR	-147.360601	64.992228
700092	Fort Knox	FTK	USA	Alaska	Orogenic - Intrusion-Related Au	Intrusion-Related Au	IR	-147.360601	64.992228
700397	Boddington	BOD	Australia	WA	Intrusion-Related	Intrusion-Related	IR	116.349488	-32.747333
700513	Westwood-Warrenmac	WWW	Canada	Quebec	Intrusion-Related	Intrusion-Related and VMS	IR	-78.502908	48.256229
700494	Canadian Malartic	CMA	Canada	Quebec	Intrusion-Related/Orogenic Au	Intrusion-Related/Orogenic Au	OGs	-78.135621	48.135039
700495	Canadian Malartic	CMA	Canada	Quebec	Intrusion-Related/Orogenic Au	Intrusion-Related/Orogenic Au	OGs	-78.135621	48.135039
700048	Co-O	COO	Phillippines	Mindano	Epithermal	Low-Sulphidation Epithermal	LSEpi	126.02829	8.241732
700051	Co-O	COO	Phillippines	Mindano	Epithermal	Low-Sulphidation Epithermal	LSEpi	126.02829	8.241732
700052	Co-O	COO	Phillippines	Mindano	Epithermal	Low-Sulphidation Epithermal	LSEpi	126.02829	8.241732
700053	Hishikari	HIS	Japan	Kagoshima	Epithermal	Low-Sulphidation Epithermal	LSEpi	130.696207	32.013132
700054	Hishikari	HIS	Japan	Kagoshima	Epithermal	Low-Sulphidation Epithermal	LSEpi	130.696207	32.013132
700055	Hishikari	HIS	Japan	Kagoshima	Epithermal	Low-Sulphidation Epithermal	LSEpi	130.696207	32.013132
700056	Creede	CRE	USA	Colorado	Epithermal	Low-Sulphidation Epithermal	LSEpi	-106.927191	37.868586
700057	Creede	CRE	USA	Colorado	Epithermal	Low-Sulphidation Epithermal	LSEpi	-106.927191	37.868586
700058	Creede	CRE	USA	Colorado	Epithermal	Low-Sulphidation Epithermal	LSEpi	-106.927191	37.868586
700151	Pajingo	PAJ	Australia	QLD	Epithermal	Low-Sulphidation Epithermal	LSEpi	146.450347	-20.526569

Table 1 continued.

Sample	Deposit Name	CharCode	Country	State	Class	SubClass	WClass	Longitude	Latitude
700207	Big Bell	BBL	Australia	WA	Orogenic Au	Orogenic Au	IR	117.6544	-27.3212
700208	Big Bell	BBL	Australia	WA	Orogenic Au	Orogenic Au	IR	117.6544	-27.3212
700082	Ridgeway	RID	Australia	NSW	Orogenic Au	Orogenic Au	OGs	148.976738	-33.436361
700083	Ridgeway	RID	Australia	NSW	Orogenic Au	Orogenic Au	OGs	148.976738	-33.436361
700084	Ridgeway	RID	Australia	NSW	Orogenic Au	Orogenic Au	OGs	148.976738	-33.436361
700085	Silver King	SIL	USA	Arizona	Orogenic Au	Orogenic Au	OGs	-111.08933	33.330743
700086	Kensington	KEN	USA	Alaska	Orogenic Au	Orogenic Au	OGs	-135.061958	58.846117
700088	Stawell	STW	Australia	VIC	Orogenic Au	Orogenic Au	OGs	142.780037	-37.054903
700089	Stawell	STW	Australia	VIC	Orogenic Au	Orogenic Au	OGs	142.780037	-37.054903
700101	Eersteling	EER	South Africa	Limpopo	Orogenic Au	Orogenic Au	OGs	29.271313	-24.121195
700102	Eersteling	EER	South Africa	Limpopo	Orogenic Au	Orogenic Au	OGs	29.271313	-24.121195
700103	Maybell	MAY	Australia	WA	Orogenic Au	Orogenic Au	OGs	121.793098	-32.370098
700104	Maybell	MAY	Australia	WA	Orogenic Au	Orogenic Au	OGs	121.793098	-32.370098
700105	Wallaby	WAL	Australia	WA	Orogenic Au	Orogenic Au	OGs	122.307714	-28.851087
700106	Wallaby	WAL	Australia	WA	Orogenic Au	Orogenic Au	OGs	122.307714	-28.851087
700113	Murchison	MUR	South Africa	Limpopo	Orogenic Au	Orogenic Au	OGs	30.686216	-23.89998
700114	Astoria	AST	Canada	Quebec	Orogenic Au	Orogenic Au	OGs	-79.025522	48.179638
700115	Crixas	CRX	Brazil	Goias	Orogenic Au	Orogenic Au	OGs	-49.964828	-14.573218
700116	Crixas	CRX	Brazil	Goias	Orogenic Au	Orogenic Au	OGs	-49.964828	-14.573218
700117	Crixas	CRX	Brazil	Goias	Orogenic Au	Orogenic Au	OGs	-49.964828	-14.573218
700118	Renco	REN	Zimbabwe	Masvingo	Orogenic Au	Orogenic Au	OGs	31.167202	-20.625731
700119	Renco	REN	Zimbabwe	Masvingo	Orogenic Au	Orogenic Au	OGs	31.167202	-20.625731
700120	Luziania	LUZ	Brazil	Goias	Orogenic Au	Orogenic Au	OGs	-48.008587	-16.233755
700121	Luziania	LUZ	Brazil	Goias	Orogenic Au	Orogenic Au	OGs	-48.008587	-16.233755
700162	Telfer	TEL	Australia	WA	Orogenic Au	Orogenic Au	OGs	122.209869	-21.721615
700190	Paddington	PDT	Australia	WA	Orogenic Au	Orogenic Au	OGs	121.3445	-30.4898
700191	Paddington	PDT	Australia	WA	Orogenic Au	Orogenic Au	OGs	121.3445	-30.4898
700192	Golden Mile	GMK	Australia	WA	Orogenic Au	Orogenic Au	OGs	121.503695	-30.77755
700193	Darlot	DLT	Australia	WA	Orogenic Au	Orogenic Au	OGs	121.269999	-27.889861
700194	Darlot	DLT	Australia	WA	Orogenic Au	Orogenic Au	OGs	121.269999	-27.889861
700195	Westonia	WTN	Australia	WA	Orogenic Au	Orogenic Au	OGs	118.698996	-31.290779
700196	Chalice	CHL	Australia	WA	Orogenic Au	Orogenic Au	OGs	121.5155	-31.8168
700197	Griffins Find	GFA	Australia	WA	Orogenic Au	Orogenic Au	OGs	118.3189	-33.0694
700198	Chalice	CHL	Australia	WA	Orogenic Au	Orogenic Au	OGs	121.5155	-31.8168
700201	Griffins Find	GFA	Australia	WA	Orogenic Au	Orogenic Au	OGs	118.3189	-33.0694
700202	Wiluna	WIL	Australia	WA	Orogenic Au	Orogenic Au	OGs	120.2386	-26.6219
700203	Wiluna	WIL	Australia	WA	Orogenic Au	Orogenic Au	OGs	120.2386	-26.6219
700204	Wiluna	WIL	Australia	WA	Orogenic Au	Orogenic Au	OGs	120.2386	-26.6219
700205	Warronga - Agnew	WGA	Australia	WA	Orogenic Au	Orogenic Au	OGs	120.5052	-28.0061
700206	Warronga - Agnew	WGA	Australia	WA	Orogenic Au	Orogenic Au	OGs	120.5052	-28.0061
700209	Hill 50	H50	Australia	WA	Orogenic Au	Orogenic Au	OGs	117.8087	-28.0429
700210	Hill 50	H50	Australia	WA	Orogenic Au	Orogenic Au	OGs	117.8087	-28.0429
700211	Lawlers	NWH	Australia	WA	Orogenic Au	Orogenic Au	OGs	120.5401	-28.0795
700212	Lawlers	NWH	Australia	WA	Orogenic Au	Orogenic Au	OGs	120.5401	-28.0795
700213	Transvaal	TVL	Australia	WA	Orogenic Au	Orogenic Au	OGs	119.3205	-31.2698

Table 1 continued.

Sample	Deposit Name	CharCode	Country	State	Class	SubClass	WClass	Longitude	Latitude
700214	Redeemer	RDM	Australia	WA	Orogenic Au	Orogenic Au	OGs	120.4833	-28.0658
700215	Macraes	MCR	New Zealand	Otago	Orogenic Au	Orogenic Au	OGs	170.4573	-45.3763
700216	Harbour lights	HBL	Australia	WA	Orogenic Au	Orogenic Au	OGs	121.3224	-28.8754
700217	Harbour lights	HBL	Australia	WA	Orogenic Au	Orogenic Au	OGs	121.3224	-28.8754
700218	Sunrise Dam	SNR	Australia	WA	Orogenic Au	Orogenic Au	OGs	122.416	-29.0808
700219	Sunrise Dam	SNR	Australia	WA	Orogenic Au	Orogenic Au	OGs	122.416	-29.0808
700220	Lindsays	LND	Australia	WA	Orogenic Au	Orogenic Au	OGs	121.1717	-30.943
700221	Three Mile Hill	3MH	Australia	WA	Orogenic Au	Orogenic Au	OGs	121.1982	-30.9264
700222	Three Mile Hill	3MH	Australia	WA	Orogenic Au	Orogenic Au	OGs	121.1982	-30.9264
700223	Three Mile Hill	3MH	Australia	WA	Orogenic Au	Orogenic Au	OGs	121.1982	-30.9264
700224	Porphyry	PRY	Australia	WA	Orogenic Au	Orogenic Au	OGs	122.2856	-29.7807
700225	Porphyry	PRY	Australia	WA	Orogenic Au	Orogenic Au	OGs	122.2856	-29.7807
700226	Jupiter	JUP	Australia	WA	Orogenic Au	Orogenic Au	OGs	122.2186	-28.8077
700227	Jupiter	JUP	Australia	WA	Orogenic Au	Orogenic Au	OGs	122.2186	-28.8077
700228	Mount Wilkinson	MWK	Australia	WA	Orogenic Au	Orogenic Au	OGs	120.2154	-26.7576
700229	Mount Wilkinson	MWK	Australia	WA	Orogenic Au	Orogenic Au	OGs	120.2154	-26.7576
700230	Golden Mile	GMK	Australia	WA	Orogenic Au	Orogenic Au	OGs	121.503695	-30.77755
700231	Golden Mile	GMK	Australia	WA	Orogenic Au	Orogenic Au	OGs	121.503695	-30.77755
700239	Karonie	KNE	Australia	WA	Orogenic Au	Orogenic Au	OGs	122.5611	-31.0346
700240	Karonie	KNE	Australia	WA	Orogenic Au	Orogenic Au	OGs	122.5611	-31.0346
700241	Karonie	KNE	Australia	WA	Orogenic Au	Orogenic Au	OGs	122.5611	-31.0346
700242	Nathans Labouchere	NLB	Australia	WA	Orogenic Au	Orogenic Au	OGs	118.31	-25.3199
700243	Micky Doolan Meekatharra	MDM	Australia	WA	Orogenic Au	Orogenic Au	OGs	118.5025	-26.6184
700254	Sheba	SHB	South Africa	Mpumalanga	Orogenic Au	Orogenic Au	OGs	31.076549	-25.733161
700263	Mount Morgans	MMG	Australia	WA	Orogenic Au	Orogenic Au	OGs	122.06944	-28.771032
700264	Golden Mile	GMK	Australia	WA	Orogenic Au	Orogenic Au	OGs	121.503695	-30.77755
700265	Golden Mile	GMK	Australia	WA	Orogenic Au	Orogenic Au	OGs	121.503695	-30.77755
700266	Golden Mile	GMK	Australia	WA	Orogenic Au	Orogenic Au	OGs	121.503695	-30.77755
700267	Kanowna Belle	KBL	Australia	WA	Orogenic Au	Orogenic Au	OGs	121.5765	-30.6112
700268	Hunt	HNT	Australia	WA	Orogenic Au	Orogenic Au	OGs	121.6802	-31.2185
700269	Marvel Loch	MVL	Australia	WA	Orogenic Au	Orogenic Au	OGs	119.4969	-31.4693
700270	Meekatharra Prohibition	MKP	Australia	WA	Orogenic Au	Orogenic Au	OGs	118.5051	-26.6047
700271	Randalls	RDL	Australia	WA	Orogenic Au	Orogenic Au	OGs	122.1993	-31.0814
700272	Randalls	RDL	Australia	WA	Orogenic Au	Orogenic Au	OGs	122.1993	-31.0814
700273	Junction	JCT	Australia	WA	Orogenic Au	Orogenic Au	OGs	121.8383	-31.4576
700274	Griffins Find	GFA	Australia	WA	Orogenic Au	Orogenic Au	OGs	118.3189	-33.0694
700275	Hunt	HNT	Australia	WA	Orogenic Au	Orogenic Au	OGs	121.6802	-31.2185
700276	Granny Smith	GSM	Australia	WA	Orogenic Au	Orogenic Au	OGs	122.4223	-28.8127
700285	Lancefield	LFD	Australia	WA	Orogenic Au	Orogenic Au	OGs	122.3813	-28.548
700286	Lancefield	LFD	Australia	WA	Orogenic Au	Orogenic Au	OGs	122.3813	-28.548
700287	Copperfield	CFD	Australia	WA	Orogenic Au	Orogenic Au	OGs	120.4658	-29.0979
700288	Hunt	HNT	Australia	WA	Orogenic Au	Orogenic Au	OGs	121.6802	-31.2185
700289	WIluna	WIL	Australia	WA	Orogenic Au	Orogenic Au	OGs	120.2386	-26.6219
700290	Youanmi	YOU	Australia	WA	Orogenic Au	Orogenic Au	OGs	119.3119	-27.9898
700383	Golden Kilometre	GKM	Australia	WA	Orogenic Au	Orogenic Au	OGs	121.236397	-30.519227

Table 1 continued.

Sample	Deposit Name	CharCode	Country	State	Class	SubClass	WClass	Longitude	Latitude
700384	Ora Banda	OBA	Australia	WA	Orogenic Au	Orogenic Au	OGs	121.064859	-30.38315
700385	Mount Charlotte	MCT	Australia	WA	Orogenic Au	Orogenic Au	OGs	121.480993	-30.746367
700386	Mount Charlotte	MCT	Australia	WA	Orogenic Au	Orogenic Au	OGs	121.480993	-30.746367
700387	Mount Charlotte	MCT	Australia	WA	Orogenic Au	Orogenic Au	OGs	121.480993	-30.746367
700388	Kanowna Belle	KBL	Australia	WA	Orogenic Au	Orogenic Au	OGs	121.576513	-30.611192
700389	Kanowna Belle	KBL	Australia	WA	Orogenic Au	Orogenic Au	OGs	121.576513	-30.611192
700390	Chalice	CHL	Australia	WA	Orogenic Au	Orogenic Au	OGs	121.515495	-31.816816
700391	Chalice	CHL	Australia	WA	Orogenic Au	Orogenic Au	OGs	121.515495	-31.816816
700392	Copperhead	CHD	Australia	WA	Orogenic Au	Orogenic Au	OGs	119.124928	-30.976901
700393	Copperhead	CHD	Australia	WA	Orogenic Au	Orogenic Au	OGs	119.124928	-30.976901
700394	Frasers	FRA	Australia	WA	Orogenic Au	Orogenic Au	OGs	119.331119	-31.239256
700395	Harlequin	HLQ	Australia	WA	Orogenic Au	Orogenic Au	OGs	121.794567	-32.114448
700396	Kings Cross	KCX	Australia	WA	Orogenic Au	Orogenic Au	OGs	121.181542	-30.952687
700398	Nevoria	NEV	Australia	WA	Orogenic Au	Orogenic Au	OGs	119.585022	-31.507187
700401	Victory	VTY	Australia	WA	Orogenic Au	Orogenic Au	OGs	121.771659	-31.323771
700402	Sons of Gwalia	SOG	Australia	WA	Orogenic Au	Orogenic Au	OGs	121.333425	-28.918846
700404	Redeemer	RDM	Australia	WA	Orogenic Au	Orogenic Au	OGs	120.48372	-28.063396
700405	Ballarat Last Chance WA	BLX	Australia	WA	Orogenic Au	Orogenic Au	OGs	121.611619	-30.596082
700426	Victory	VTY	Australia	WA	Orogenic Au	Orogenic Au	OGs	121.771659	-31.323771
700427	Nevoria	NEV	Australia	WA	Orogenic Au	Orogenic Au	OGs	119.585022	-31.507187
700492	Salt Creek	SCK	Australia	WA	Orogenic Au	Orogenic Au	OGs	122.0206183	-31.1083
700493	Beaufor	BFR	Canada	Quebec	Orogenic Au	Orogenic Au	OGs	-77.555914	48.159333
700496	Detour Lake	DTL	Canada	Ontario	Orogenic Au	Orogenic Au	OGs	-79.718391	50.017776
700497	Detour Lake	DTL	Canada	Ontario	Orogenic Au	Orogenic Au	OGs	-79.718391	50.017776
700498	Dome Mine	DOM	Canada	Ontario	Orogenic Au	Orogenic Au	OGs	-81.241391	48.462964
700501	Dome Mine	DOM	Canada	Ontario	Orogenic Au	Orogenic Au	OGs	-81.241391	48.462964
700502	Francoeur	FCR	Canada	Quebec	Orogenic Au	Orogenic Au	OGs	-79.275215	48.158702
700503	Giant	GIA	Canada	NWT	Orogenic Au	Orogenic Au	OGs	-114.359302	62.499779
700504	Lac Herbin	LHB	Canada	Quebec	Orogenic Au	Orogenic Au	OGs	-77.650808	48.134823
700505	Meadowbank	MDB	Canada	Nunavut	Orogenic Au	Orogenic Au	OGs	-96.070482	65.021028
700506	Musselwhite	MSW	Canada	Ontario	Orogenic Au	Orogenic Au	OGs	-90.366311	52.611458
700507	Meliadine Tiriganiaq deposit	MTG	Canada	Nunavut	Orogenic Au	Orogenic Au	OGs	-92.17885	63.027055
700508	Pine Cove	PCV	Canada	Newfoundland	Orogenic Au	Orogenic Au	OGs	-56.130003	49.959586
700509	Rice Lake	RLK	Canada	Manitoba	Orogenic Au	Orogenic Au	OGs	-95.675197	51.021385
700510	Rice Lake	RLK	Canada	Manitoba	Orogenic Au	Orogenic Au	OGs	-95.675197	51.021385
700511	Timmins West	TMW	Canada	Ontario	Orogenic Au	Orogenic Au	OGs	-81.557712	48.390235
700512	Thunder Creek	TCK	Canada	Ontario	Orogenic Au	Orogenic Au	OGs	-81.55185	48.384038
700097	Hemlo Williams	HWL	Canada	Ontario	Intrusion-Related Au	Transition Intrusion-Related to Epithermal	IR	-85.92856	48.697006
700098	Hemlo Williams	HWL	Canada	Ontario	Intrusion-Related Au	Transition Intrusion-Related to Epithermal	IR	-85.92856	48.697006

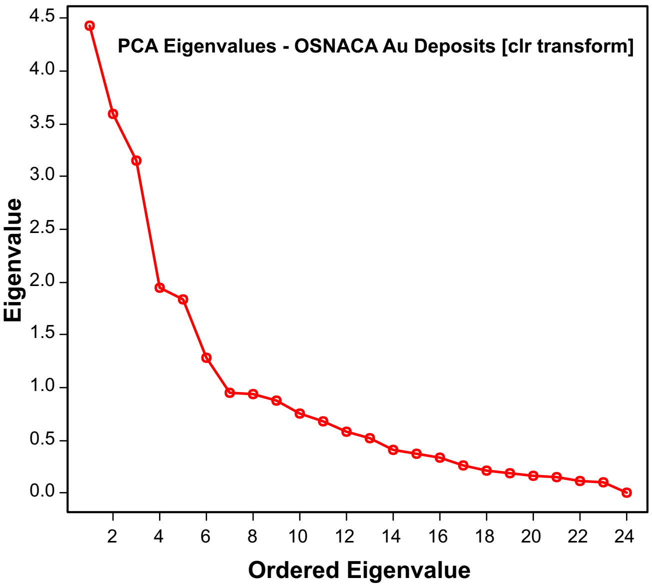

Figure 1. Screeplot of order eigenvalues derived from centred log-transformed geochemical data from the database of three types of gold deposits.

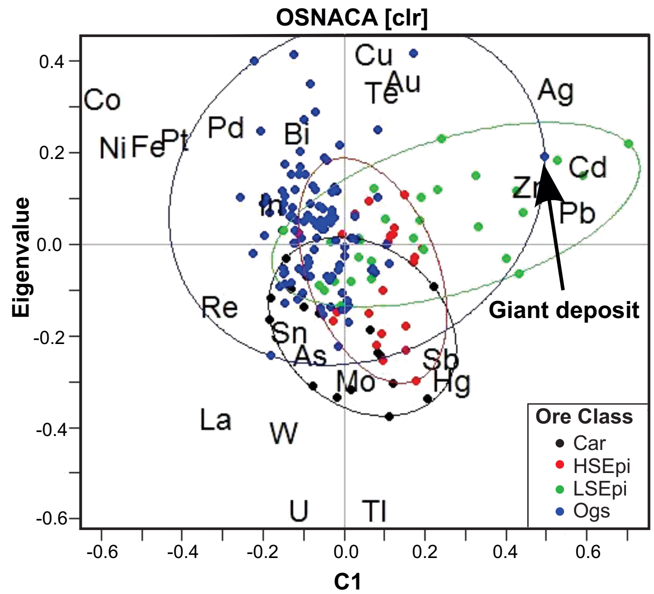

Figure 2. Biplot of principal components PC1 and PC2 for the four gold deposit types. The loadings of the elements are scaled to fit on the same diagram as the scores of the individual samples (observations). A convex ellipsoid hull encompasses the range of values for each gold deposit type and enhances the view of overlap and range. The Giant deposit (Yellowknife, Canada) is shown because of its distinct departure from the other orogenic greenstone-hosted gold deposits. See text for more details on the significance of the elements and observations. Abbreviations: Car = Carlin; HSEpi = high-sulphidation epithermal; LSEpi = low-sulphidation epithermal; OGs = orogenic greenstone-hosted.

The methods used in this study were applied in the R programming environment (R Core Team, 2014).

The data were then transformed using a centred log-ratio, as documented by Aitchison (1986) and others (Egozcue et al., 2003; Buccianti et al., 2006; Pawlowsky and Buccianti, 2011). The use of log-ratios overcomes the problem of data closure (constituents summing to a constant) and opens the data into the real number space rather than being confined to the positive number space, known as the simplex. This transformation permits the application of standard statistical methodology.

Process Discovery

A principal component analysis (PCA) was applied to the log-centred (clr) data. The results are shown in Table 2 and Figures 1 and 2. Table 2 shows that the first 8 components account for more than 76% of the variation of the data. The R-scores provide the coordinates of the elements on the biplots (Fig. 2). The relative contributions indicate the percentage that each component contributes to the variability of a specific element. The absolute contributions indicate the percentage that each element contributes to a given component. The first three components account for 47% of the data variability. As Figure 2 illustrates, there are distinct element associations with specific deposit types. The low-sulphidation (LSEpi) gold deposits show a contrast of relative enrichment of Ag-Cd-Zn-Pb at a sub-horizontal angle to the PC1 axis. High-sulphidation epithermal deposits are associated with relative enrichment in Sb-Hg-As-Sn-Mo. Carlin-type gold deposits yield relatively low PC2 scores, which correspond to As-Sn-Sb-Hg (key geochemical signature) and also Mo-U-Tl-W-La-Re element assemblages. Orogenic greenstone-hosted (OGs) gold deposits show a range of relative enrichment in Co-Ni-Fe-Pt-Pd-Cu-Te, which likely represents a mafic host-rock association, as seen along the positive PC2 axis. There is a corresponding relative depletion of these elements towards the origin of the figure. These trends require more detailed interpretation within the context of the geology of the deposits, which is beyond the scope of this initial study. It is also important to note that there is significant overlap between ore geochemistry at each of the deposit types. This is emphasized through the addition of ellipses (convex hulls) around the range of the samples that define each class. As noted in Figure 2, the. Giant gold mine, (Yellowknife, Northwest Territories, Canada) appears to have a closer association with low-sulphidation epithermal deposits.

Another method for investigating the dominant associations and trends in multivariate data is multidimensional scaling (MDS). This method (see Venables and Ripley, 2002, p. 306) provides a measure of optimum distribution of observations within a defined dimensional space. Typically MDS is rendered in two or three dimensions. Figure 3 shows a plot of the two MDS coordinates derived from the application of a two-dimensional MDS. As in the PCA biplot of Figure

Table 2. Summary of principal component analysis. Only the first 10 principal components are shown (for brevity). See text for detailed explanation. R-scores are contrasted by red (values > 0) and blue (<=0). Bold red values are highlighted for relative and absolute contributions of >10.

Eigenvalues

	PC1	PC2	PC3	PC4	PC5	PC6	PC7	PC8	PC9	PC10
λ	4.4400	3.5900	3.1500	1.9500	1.8400	1.2900	0.9500	0.9400	0.8700	0.7600
$\lambda\%$	18.6085	15.0461	13.2020	8.1727	7.7117	5.4065	3.9816	3.9396	3.6463	3.1852
$\Sigma\lambda\%$	18.6085	33.6547	46.8567	55.0293	62.7410	68.1475	72.1291	76.0687	79.7150	82.9003

R-Scores

	PC1	PC2	PC3	PC4	PC5	PC6	PC7	PC8	PC9	PC10
Fe	-0.6057	0.2705	-0.2491	0.0321	0.1320	-0.4479	0.1137	0.0682	0.0877	-0.1391
Co	-0.7469	0.4000	-0.1807	0.0404	0.0642	-0.1777	0.0399	-0.0472	0.1164	-0.2642
Ni	-0.7142	0.2673	0.2863	-0.0418	0.1590	0.1361	0.0670	0.1424	-0.0294	-0.3238
Re	-0.3826	-0.1658	-0.0975	-0.4794	0.1884	0.0582	0.1820	0.2725	0.3888	0.4057
Pd	-0.3626	0.3248	0.5970	0.1969	0.2231	0.3764	0.0552	-0.1102	-0.0165	0.2151
Pt	-0.5223	0.2873	0.5323	0.2311	0.2268	0.3423	0.0158	-0.1298	-0.0250	0.1284
Cu	0.0952	0.5227	-0.3013	0.3836	-0.3489	0.0529	0.1331	0.2299	0.2179	-0.0315
Ag	0.6588	0.4180	0.0538	-0.3261	-0.0003	0.0307	0.1611	-0.1434	-0.0466	0.0762
Au	0.1872	0.4497	0.2756	-0.5640	-0.0739	-0.0744	-0.0485	-0.1793	-0.2896	0.0490
Zn	0.5792	0.1586	-0.2824	0.2692	0.5404	-0.1806	0.0129	-0.0259	0.1011	0.0002
Cd	0.7557	0.2160	-0.1240	0.2514	0.3568	0.0060	0.0165	0.0055	0.1557	0.0473
In	-0.2216	0.1121	-0.4959	0.3661	-0.2864	-0.1586	0.1870	-0.2907	-0.1355	0.1819
Tl	0.0956	-0.7251	0.2283	-0.0501	0.0168	0.1325	-0.1298	-0.1821	0.0784	-0.2967
Pb	0.7207	0.0912	-0.2095	0.2182	0.2768	0.1738	0.1581	0.0843	-0.1874	-0.2019
Hg	0.3355	-0.3795	0.3856	-0.1107	-0.3312	0.1252	0.0402	-0.0985	0.4332	-0.2718
As	-0.1003	-0.3007	0.5099	0.3136	-0.1071	-0.5296	-0.2433	0.2708	-0.1567	0.0781
Sb	0.3028	-0.3097	0.5956	0.2421	-0.3443	-0.1591	0.0683	0.2077	-0.1487	0.1752
Bi	-0.1435	0.3058	-0.4965	-0.0128	-0.3824	0.4169	-0.2037	0.2026	-0.3276	-0.0929
Te	0.1198	0.4179	-0.1621	-0.4972	-0.0882	-0.2296	-0.4539	-0.2100	0.1043	0.0414
Mo	0.0366	-0.3698	-0.4133	-0.4509	-0.0757	0.1296	0.2215	0.4135	-0.1139	-0.0013
W	-0.1838	-0.5108	-0.0411	-0.1409	-0.0901	-0.1603	0.5571	-0.3489	-0.1948	-0.0409
Sn	-0.1671	-0.2383	-0.4707	0.2953	-0.4907	0.1876	-0.1348	-0.2534	0.2105	0.1777
La	-0.3954	-0.4726	-0.4215	0.0031	0.4547	-0.0209	-0.1541	-0.1138	-0.1249	0.0914
U	-0.1374	-0.7247	-0.3332	0.0776	0.3106	0.1772	-0.2340	0.0117	-0.0927	0.0337

Relative Contributions

	PC1	PC2	PC3	PC4	PC5	PC6	PC7	PC8	PC9	PC10
Fe	**36.8961**	7.3601	6.2390	0.1035	1.7536	**20.1776**	1.2989	0.4674	0.7731	1.9446
Co	**56.0980**	**16.0885**	3.2824	0.1644	0.4139	3.1753	0.1605	0.2244	1.3621	7.0223
Ni	**51.2935**	7.1848	8.2419	0.1756	2.5425	1.8632	0.4520	2.0387	0.0871	**10.5459**
Re	**14.7209**	2.7656	0.9555	**23.1103**	3.5697	0.3409	3.3322	7.4675	**15.2037**	**16.5546**
Pd	**13.2194**	**10.6078**	**35.8478**	3.8986	5.0061	**14.2458**	0.3066	1.2222	0.0275	4.6515
Pt	**27.4363**	8.2987	**28.4927**	5.3729	5.1719	**11.7814**	0.0250	1.6930	0.0628	1.6573
Cu	0.9114	**27.4797**	9.1274	**14.7951**	**12.2451**	0.2819	1.7828	5.3158	4.7768	0.0999
Ag	**43.6405**	**17.5695**	0.2916	**10.6970**	0.0000	0.0947	2.6101	2.0679	0.2183	0.5841
Au	3.5227	**20.3418**	7.6367	**31.9926**	0.5495	0.5565	0.2362	3.2348	8.4320	0.2414
Zn	**33.7380**	2.5307	8.0203	7.2867	**29.3664**	3.2813	0.0168	0.0675	1.0287	0.0000
Cd	**57.4243**	4.6938	1.5456	6.3582	**12.8003**	0.0037	0.0274	0.0031	2.4385	0.2247
In	4.9404	1.2631	**24.7333**	**13.4814**	8.2492	2.5298	3.5163	8.4967	1.8471	3.3272
Tl	0.9183	**52.8799**	5.2408	0.2529	0.0283	1.7663	1.6954	3.3351	0.6175	8.8517
Pb	**52.2297**	0.8359	4.4122	4.7882	7.7036	3.0372	2.5135	0.7139	3.5310	4.0984
Hg	**11.3214**	**14.4830**	**14.9514**	1.2322	**11.0324**	1.5751	0.1623	0.9756	**18.8708**	7.4274
As	1.0108	9.0923	**26.1518**	9.8895	1.1536	**28.2057**	5.9512	7.3733	2.4685	0.6133
Sb	9.2230	9.6439	**35.6756**	5.8928	**11.9221**	2.5455	0.4686	4.3379	2.2241	3.0852
Bi	2.0716	9.4052	**24.7923**	0.0166	**14.7085**	**17.4775**	4.1731	4.1295	**10.7954**	0.8683
Te	1.4432	**17.5625**	2.6430	**24.8611**	0.7828	5.2993	**20.7187**	4.4356	1.0939	0.1722
Mo	0.1349	**13.7519**	**17.1817**	**20.4421**	0.5764	1.6885	4.9323	**17.1936**	1.3035	0.0002
W	3.3990	**26.2442**	0.1702	1.9961	0.8173	2.5850	**31.2069**	**12.2404**	3.8160	0.1680
Sn	2.8071	5.7124	**22.2772**	8.7668	**24.2112**	3.5376	1.8263	6.4560	4.4577	3.1748
La	**15.7205**	**22.4624**	**17.8642**	0.0010	**20.7918**	0.0438	2.3870	1.3018	1.5692	0.8404
U	1.8995	**52.8104**	**11.1639**	0.6056	9.6994	3.1587	5.5061	0.0138	0.8644	0.1145

Absolute Contributions

	PC1	PC2	PC3	PC4	PC5	PC6	PC7	PC8	PC9	PC10
Fe	8.2723	2.0384	1.9685	0.0527	0.9474	**15.6110**	1.3629	0.4930	0.8798	2.5497
Co	**12.5774**	4.4558	1.0357	0.0838	0.2236	2.4567	0.1684	0.2367	1.5502	9.2074
Ni	**11.5002**	1.9899	2.6005	0.0895	1.3736	1.4415	0.4743	2.1504	0.0991	**13.8274**
Re	3.3005	0.7660	0.3015	**11.7801**	1.9286	0.2637	3.4963	7.8766	**17.3025**	**21.7059**
Pd	2.9639	2.9379	**11.3107**	1.9872	2.7046	**11.0217**	0.3217	1.2892	0.0313	6.0990
Pt	6.1513	2.2984	8.9900	2.7387	2.7942	9.1151	0.0262	1.7858	0.0715	2.1730
Cu	0.2043	7.6107	2.8799	7.5415	6.6156	0.2181	1.8706	5.6071	5.4362	0.1310
Ag	9.7844	4.8660	0.0920	5.4526	0.0000	0.0732	2.7387	2.1812	0.2485	0.7659
Au	0.7898	5.6338	2.4095	**16.3077**	0.2969	0.4305	0.2479	3.4120	9.5960	0.3165
Zn	7.5642	0.7009	2.5306	3.7143	**15.8655**	2.5387	0.0176	0.0712	1.1707	0.0000
Cd	**12.8748**	1.3000	0.4877	3.2410	6.9155	0.0028	0.0287	0.0032	2.7751	0.2946
In	1.1077	0.3498	7.8038	6.8719	4.4567	1.9572	3.6895	8.9622	2.1021	4.3626
Tl	0.2059	**14.6454**	1.6536	0.1289	0.0153	1.3665	1.7789	3.5179	0.7028	**11.6060**
Pb	**11.7101**	0.2315	1.3921	2.4407	4.1619	2.3498	2.6373	0.7530	4.0184	5.3737
Hg	2.5383	4.0112	4.7174	0.6281	5.9604	1.2187	0.1703	1.0291	**21.4759**	9.7386
As	0.2266	2.5182	8.2514	5.0410	0.6232	**21.8222**	6.2442	7.7773	2.8093	0.8042
Sb	2.0678	2.6709	**11.2563**	3.0038	6.4410	1.9694	0.4917	4.5756	2.5312	4.0453
Bi	0.4645	2.6048	7.8224	0.0085	7.9464	**13.5220**	4.3787	4.3558	**12.2857**	1.1384
Te	0.3236	4.8641	0.8339	**12.6725**	0.4229	4.1000	**21.7391**	4.6786	1.2449	0.2257
Mo	0.0302	3.8087	5.4212	**10.4200**	0.3114	1.3064	5.1752	**18.1357**	1.4835	0.0002
W	0.7621	7.2685	0.0537	1.0175	0.4415	2.0000	**32.7438**	**12.9111**	4.3428	0.2203
Sn	0.6294	1.5821	7.0289	4.4687	**13.0804**	2.7369	1.9163	6.8098	5.0731	4.1627
La	3.5246	6.2211	5.6365	0.0005	**11.2330**	0.0339	2.5045	1.3732	1.7858	1.1019
U	0.4259	**14.6262**	3.5224	0.3087	5.2402	2.4438	5.7772	0.0146	0.9837	0.1501

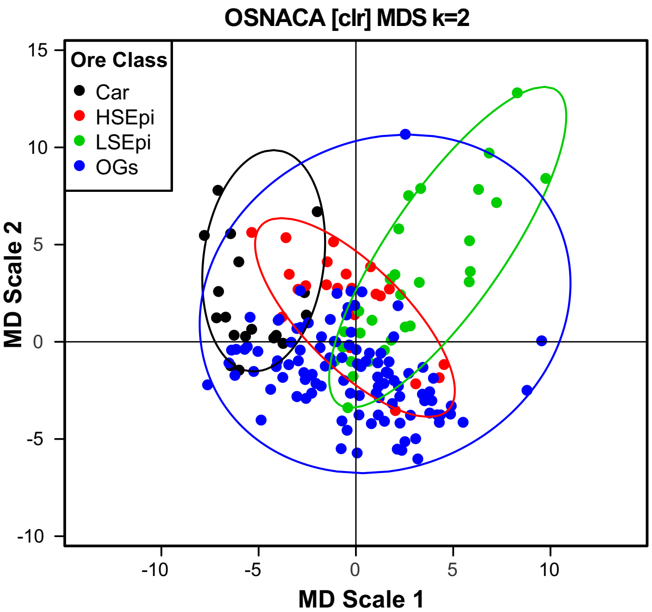

Figure. 3. Multidimensional scaling plot of reduced dimensionality of the data (2 dimensions). As in Figure 2, the overlap and relationship between the four gold deposit classes is enhanced by convex ellipsoid hulls that encompass each deposit type. Abbreviations: Car = Carlin; HSEpi = high-sulphidation epithermal; LSEpi = low-sulphidation epithermal; OGs = orogenic greenstone-hosted.

2, there is significant overlap of the four classes. The extended range of the orogenic greenstone-hosted (OGs) deposits is due to three individual deposits shown in the figure: one of which is the Giant gold mine, discussed previously. The chemistry of these three deposits may be different due to wall-rock contamination or they have been misclassified. Similarly, three Carlin-type deposits occur within the field dominated by high-sulphidation epithermal deposits. This overlap may be the result of misclassification or an insufficient range of Carlin-type deposit geochemistry. However, these deposit types share some analogies in terms of low-pH fluid chemistry and strong silicification (jasperoid versus massive silica), which may explain at least part of the geochemical overlap. Several of the deposits are close to the origin of the plot, suggesting that they are compositionally similar and highlights the fact that knowledge of the geology of the deposits and the associated paragenesis is critical in characterizing and classifying gold deposits.

Process Validation

Assessing the statistical uniqueness of the gold deposit types can be performed through an analysis of variance (Venables and Ripley, 2002). The four types of gold deposits were subjected to an analysis of variance, based on the centred log-transformed data and the principal component scores derived from the centred log-transform of the data. A graphical summary of the results are shown in Figures 4 and 5. Figure 4 shows

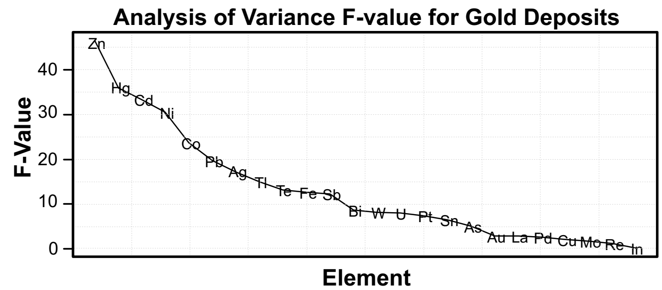

Figure 4. Ordered plot of F-values for each element based on analysis of variance on log centred transform geochemical data for each of the four gold deposit types. High F-values indicate better group separability. Co and Cd are better at discriminating between the four gold deposits types, whereas Sn and Mo are poor at discriminating between the types of gold deposits.

that Zn-Hg-Cd-Ni-Co-Pb-Ag-Tl-Te-Fe-Sb account for most of the discriminating power between the three of the deposit types. Since all deposits contain Au, it is expected to see that Au has low discriminating power. Figure 5 shows the results of a discriminant analysis applied to the principal components. In contrast to Figure 4, principal components 1, 5, and 2 account for most of the discriminating power between the four deposit types. Table 2 shows that both the relative and absolute contributions to PC5 are dominated by Zn (low-temperature Au deposition?). Since principal components represent linear combinations of the elements, they can typically reflect the stoichiometric controls that govern the associations of the minerals. These linear combinations result in fewer numbers of variables being required to define the variation in the data. In this case, the three principal components listed above (principal components 1, 5, and 2) are sufficient for the purposes of classification of the gold deposits.

An interesting feature of the multi-element chemistry of the gold deposits included in this study is the dominance of Zn as a significant element in defining deposit class separation (Fig. 4). This implies that Zn may represent a proxy for the deposition of Au in low-temperature environments.

The four groups of deposit types were classified using a linear discriminant procedure (lda, see Venables and Ripley, 2002). Cross-validation procedures (e.g. Venables and Ripley, 2002, section 12.6) were used, which sampled the dataset 20 times, from which average classification accuracy was established. The results of this classification are shown in Table 3. The overall classification accuracy is 80.9%, with individual class accuracies ranging from 50.0 to 96.3%. Overlap and/or misclassification are shown in the off-diagonal elements of the accuracy matrix of Table 3. Carlin-type (Car) deposits show overlap/misclassification with high-sulphidation epithermal (HSEpi) deposits and orogenic greenstone-hosted (OGs)

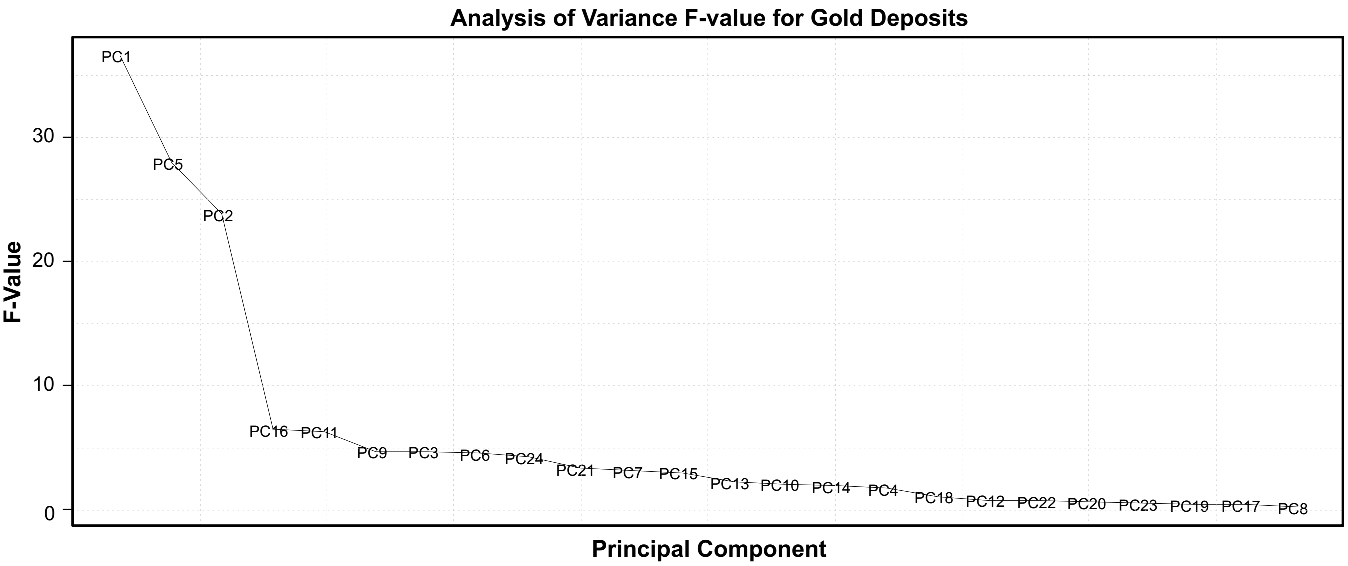

Figure. 5. Ordered plot of F-values for each principal component based on analysis of variance for the four types of gold deposits. High F-values indicate better group separability. The plot shows that PC1 and PC2 are much better at discriminating between the four types of gold deposits than any of the other components.

deposits. High-sulphidation epithermal (HSEpi) deposits show overlap/misclassification with Carlin-type, and orogenic greenstone-hosted deposits. Low-sulphidation epithermal gold deposits show overlap with orogenic greenstone-hosted deposits. Orogenic greenstone-hosted deposits show overlap with all of the other classes and intrusion-related deposits show minor overlap/misclassification with orogenic greenstone-hosted gold deposits. These associations are graphically shown in Figure 6 as a plot of the first two linear discriminant scores. The colour of each observation defines the deposit class to which the sample was initially assigned. The symbol defines the class to which each observation from the linear discriminant procedure was assigned. All four deposit classes occupy unique regions of the plot. The convex hull ellipsoid provides a measure of the overlap between the classes after the classification by the "lda" procedure. The "misclassification" of the Giant deposit is highlighted in this figure.

DISCUSSION

The methodology presented here provides a framework in which high-quality geochemical data from a database of ore geochemistry can be used for characterizing well known mineral deposit types. The results presented in this study are restricted to four types of gold deposits. Other types of gold deposits (e.g. skarn, porphyry, volcanic-hosted, paleoplacer) can be studied as well. The methods employed in this study are based solely on geochemistry and the resulting overlap between classes and apparent misclassification (e.g. Giant deposit) indicates that geochemistry alone is

Table 3. Accuracy of the prediction of gold deposit types based on a 20-fold cross-validation linear discriminant analysis.

	Count Accuracy				% Accuracy			
	Car	HSEpi	LSEpi	OGs	Car	HSEpi	LSEpi	OGs
Car	11	1	0	6	61.11	5.56	0	33.33
HSEpi	4	11	0	7	18.18	50.00	0	31.82
LSEpi	0	0	17	12	0	0	58.62	41.38
OGs	1	2	1	105	0.92	1.83	0.92	96.33

Overall Accuracy (%) 80.9

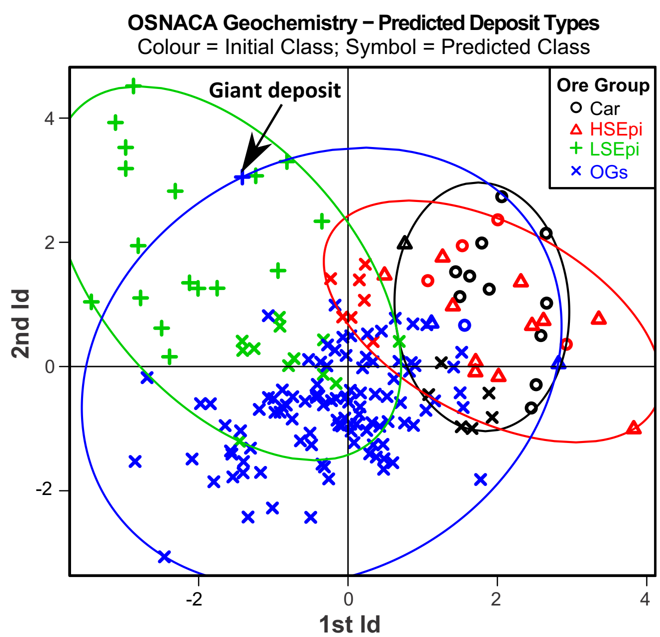

Figure 6. Plot of linear discriminant scores 1 and 2 for the three types of gold deposits. The linear discriminant scores were determined from the principal components shown in Figure 5, namely: PC1, PC5, and PC2. See Table 3 for the accuracy of the linear discriminant model. Abbreviations: Car = Carlin; HSEpi = high-sulphidation epithermal; LSEpi = low-sulphidation epithermal; OGs = orogenic greenstone-hosted.

insufficient to uniquely classify ore deposits. Hodgson and Troop (1988) provide details on criteria for gold deposit exploration based on computer based methods using a database of key gold deposit characteristics. Studies by Drew and Menzie (1993) detail the importance of the regional geological/tectonic framework in defining metrics for ore-deposit classification. Poulsen et al. (2000) provide a decision tree based on geological characteristics that can helpful to classify the gold deposit type. Our results suggest that ore geochemistry can support these classifications schemes and also highlight that ore deposits clans define a "magmato-hydrothermal space".

IMPLICATIONS FOR EXPLORATION

The approach used in this study demonstrates the geochemical distinctiveness of the major types of gold deposits derived from a global database of ore deposits. Despite demonstrated overlap between the four gold deposit types studied herein, the framework establishes a baseline for testing unknown samples for the potential affinity with the environments of gold deposit formation.

Currently, the OSNACA database does not have sufficient numbers of representative ore sample chemistry for the less common mineral deposit types, which creates difficulty when applying statistical methods. An ongoing study at the Centre for Exploration Technology, University of Australia, is involved in the characterization and classification of a broader suite of mineral deposits. Preliminary results (Grunsky et al., 2013) show that a consistent methodological approach together with carefully chosen ore-deposit samples and exacting laboratory standards and protocols will create a reliable database that can be used for a variety of research and mineral exploration purposes.

FUTURE WORK

Further work is required to gather more data from the global inventory of ore-deposit samples and research more detailed relationships within the data. As the database grows, both the distinctiveness and overlap that exists as a continuum between gold deposits will evolve and become more refined. A continuum of other ore deposit styles, i.e., the magmato-hydrothermal space, is the subject for further study. These data are also available from the OSNACA database and may be used for future studies.

ACKNOWLEDGEMENTS

Support from the Targeted Geoscience Initiative 4 – Gold Deposits, the Centre for Exploration Technology, University of Western Australia and SIPA Resources, Perth, Australia is gratefully acknowledged. The authors wish to thank Chris Lawley for his thoughtful and helpful review of the manuscript.

REFERENCES

Aitchison, J., 1986. The statistical analysis of compositional data. Monographs on statistics and applied probability; Chapman & Hall Ltd., London, 416 p.

Brauhart, C.W., Grunsky, E.C., Hagemann, S., and Dubé, B., 2015. OSNACA Project website, Centre for Exploration Technology, University of Western Australia, Australia, http://www.cet.edu.au/research-projects/special-projects/projects/osnaca-ore-samples-normalised-to-average-crustal-abundance.

Buccianti, A., Mateu-Figueras, G., and Pawlowsky-Glahn, V., 2006. Compositional Data Analysis in the Geosciences: From Theory to Practice; Geological Society, Special Publication 264, 212 p.

Drew, L.J. and Menzie, D.W., 1993; Is there a metric for mineral deposit occurrence probabilities?; Nonrenewable Resources, v. 2, p. 92–105.

Egozcue, J.J., Pawlowsky-Glahn, V., Mateu-Figueras, G., and Barcelo-Vidal, C., 2003. Isometric Logratio Transformations for Compositional Data Analysis; Mathematical Geology, v. 35, p. 279–300.

Groves, D.I., Bierlein, F.P., Meinert, L.D., and Hitzman M.W., 2010. Iron Oxide Copper-Gold (IOCG) deposits through Earth history: Implications for origin, lithospheric setting, and distinction from other epigenetic iron oxide deposits; Economic Geology, v. 105, p. 641–654.

Grunsky, E.C., Brauhart, C., Mueller, U., Dubé, B., and Hagemann, S., 2013. Ore samples normalized to average crustal abundance (OSNACA): a global online database and a new technique for quantifying multi-element ore deposit signatures; PDAC-SEG Canada Student Chapter Minerals Colloquium, Prospectors and Developers Association of Canada Meeting, March 4, 2013, poster.

Hannington, M.D., Poulsen, K.H., Thompson, J.F.H., and Sillitoe, R.H., 1999. Volcanogenic gold in the massive sulfide environment, *In:* Volcanic-Associated Massive Sulfide Deposits: Processes and Examples in Modern and Ancient Settings, (ed.) C.T. Barrie and M.D. Hannington; Society of Economic Geologists, Reviews in Economic Geology 8, p. 325–356.

Hodgson, C.J. and Troop, D.G., 1988. A new computer-aided methodology for area selection in gold exploration: a case study from the Abitibi Greenstone Belt, Ontario; Economic Geology, v. 83, p. 952–977.

Leach, D.L., Sangster, D.F., Kelley, K.D., Large, R.R., Garven, G., Allen, C.R., Gutzmer, J., and Walters, S.G., 2005. Sediment-hosted lead-zinc deposits: A global perspective, *In:* 100th Anniversary Volume, (ed.) J.W. Hedenquist, J.F.H. Thompson, R.J. Goldfarb, and J.P. Richards; Society of Economic Geologists, v. 40, p. 561–607.

Nesbitt, B.E., 1988. Gold deposit continuum: A genetic model for lode Au mineralization in the continental crust; Geology, v. 16, p. 1044–1048.

OSNACA, 2013. OSNACA: Ore samples normalized to average crustal abundance, http://www.cet.edu.au/research-projects/special-projects/projects/osnaca-ore-samples-normalised-to-average-crustal-abundance.

Palarea-Albaladejo J. and Martin-Fernandez J.A., 2008. A modified EM alr-algorithm for replacing rounded zeros in compositional data sets; Computers & Geosciences, v. 34, p. 902–917

Pawlowsky-Glahn, V. and Buccianti, A. (ed.), 2011. Compositional Data Analysis, Theory and Applications; Wiley & Sons, New York, 378 p.

Poulsen, K.H., Robert, F., and Dubé, B., 2000. Geological classification of Canadian gold deposits; Geological Survey of Canada, Bulletin 540, 106 p.

R Core Team, 2014. R: A language and environment for statistical computing; R Foundation for Statistical Computing, Vienna, Austria. URL (http://www.R-project.org/).

Sillitoe, R.H., 1989. Gold deposits in western Pacific island arcs: The magmatic connection, *In:* The Geology of Gold Deposits: The Perspective in 1988, (ed.) R.R. Keays, W.R., Ramsay, and D.I. Groves; Society of Economic Geologist, Monograph 6, p. 274–291.

Venables, W.N. and Ripley, B.D., 2002. Modern Applied Statistics with S (Fourth Edition); Springer, Berlin, 495 p.

Appendix

Refereed Publications Related to theTGI-4 Lode Gold Ore Systems Project

PUBLICATIONS IN SCIENTIFIC JOURNALS

Dubé, B., Mercier-Langevin, P., Kjarsgaard, I., Hannington, M., Bécu, V., Côté, J., Moorhead, J., Legault, M., and Bédard, N. 2014. The Bousquet 2-Dumagami world-class Archean Au-rich volcanogenic massive sulfide deposit, Abitibi, Quebec: metamorphosed submarine advanced argillic alteration footprint and genesis, *In:* A Special Issue on Archean Magmatism, Volcanism, and Ore Deposits – Part 2; Economic Geology, v. 109, p. 121–166. doi:10.2113/econgeo.109.1.121

Lawley, C.J.M., Creaser, R., Jackson, S., Yang, Z., Davis, B., Pehrsson, S., Dubé, Mercier-Langevin, P., and Vaillancourt, D., submitted. Unravelling the Western Churchill Province Paleoproterozoic gold metallotect: constraints from Re-Os arsenopyrite and U-Pb xenotime geochronology and LA-ICP-MS arsenopyrite geochemistry at the BIF-hosted Meliadine gold district, Nunavut, Canada; Economic Geology.

Lawley, C.J.M., Dubé, B., Mercier-Langevin, P., Kjarsgaard, B., Knight, R., and Vaillancourt, D., in press. Defining and mapping hydrothermal footprints at the BIF-hosted Meliadine Gold District, Nunavut, Canada; Journal of Geochemical Exploration. Available online.

McNicoll, V., Dubé, B., Castonguay, S., Oswald, W., Biczok, J., Mercier-Langevin, P., Skulski, T., and Malo, M., submitted. The world-class Musselwhite BIF-hosted gold deposit, Superior Province, Canada: new high-precision U-Pb geochronology and implications for the geological and structural setting of the deposit and gold exploration; Precambrian Research.

Mercier-Langevin, P., Hannington, M.D., Dubé, B. and Bécu, V., 2011. The gold content of volcanogenic massive sulfide deposits; Mineralium Deposita, v. 46, p. 509–539. doi:10.1007/s00126-010-0300-0

Mercier-Langevin, P., Houlé, M.G., Dubé, B., Monecke, T., Hannington, M.D., Gibson, H.L., and Goutier, J., 2012. A special issue on Archean magmatism, volcanism, and ore deposits: Part 1. Komatiite-associated Ni-Cu-(PGE) sulfide and greenstone-hosted Au deposits — Preface; Economic Geology, v. 107, p. 745–753. doi:10.2113/econgeo.107.5.745

Mercier-Langevin, P., Daigneault, R., Goutier, J., Dion, C., and Archer, P., 2012. Geology of the Archean intrusion-hosted La-Grande-Sud Au-Cu Prospect, La Grande Subprovince, James Bay Region, Québec, *In:* A Special Issue on Archean Magmatism, Volcanism, and Ore Deposits – Part 1; Economic Geology, v. 107, p. 935–962. doi:10.2113/econgeo.107.5.935

Mercier-Langevin, P., McNicoll, V., Allen, R., Blight, J., and Dubé, B., 2013. The Boliden gold-rich volcanogenic massive sulfide deposit, Skellefte District, Sweden: new U-Pb age constraints and implications at deposit and district scale; Mineralium Deposita, v.48, p. 485–504. doi:10.1007/s00126-012-0438-z

Mercier-Langevin, P., Lafrance, B., Bécu, V., Dubé, B., Kjarsgaard, I., and Guha, J., 2014. The Lemoine auriferous volcanogenic massive sulfide deposit, Chibougamau camp, Abitibi greenstone belt, Québec, Canada: geology and genesis, *In:* A Special Issue on Archean Magmatism, Volcanism, and Ore Deposits – Part 2; Economic Geology, v. 109, p. 231–269. doi:10.2113/econgeo.109.1.231

GOVERNMENT REPORTS

Bleeker, W., 2012. Targeted Geoscience Initiative 4. Lode gold deposits in ancient deformed and metamorphosed terranes: the role of extension in the formation of Timiskaming Basins and large gold deposits, Abitibi Greenstone Belt—A discussion, *In:* Summary of Field Work and other Activities 2012; Ontario Geological Survey, Open File Report 6280, p. 47-1 to 47-12.

Bleeker, W., Atkinson, B.T., and Stalker, M., 2014. A "New" Occurrence of Timiskaming sedimentary rocks in the Northern Swayze Greenstone Belt, Abitibi Subprovince—with implications for the western continuation of the Porcupine–Destor Fault Zone and nearby gold mineralization, *In:* Summary of Field Work and Other Activities 2014; Ontario Geological Survey, Open File Report 6300, p. 43-1 to 43-10.

Dubé, B., Mercier-Langevin, P., Castonguay, S., McNicoll, V.J., Pehrsson, S.J., Bleeker, W., Schetselaar, E.M., and Jackson, S., 2011. TGI-4 lode gold deposits in ancient, deformed and metamorphosed terranes – footprints and exploration implications: a preliminary overview of themes, objectives and targeted areas, *In:* Summary of Field Work and other Activities 2011; Ontario Geological Survey, Open File Report 6270, p. 38-1 to 38-10.

Gourcerol, B., Thurston, P., Kontak, D.J., and Côté-Mantha, O., 2014. Interpretations and implications of preliminary LA ICP-MS analysis of chert for the origin of geochemical signatures in banded iron-formations (BIFs)

Appendix: Refereed publications related to the TGI-4 Lode Gold Ore Systems Project, *In:* Targeted Geoscience Initiative 4: Contributions to the Understanding of Precambrian Lode Gold Deposits and Implications for Exploration, (ed.) B. Dubé and P. Mercier-Langevin; Geological Survey of Canada, Open File 7852, p. 287–293.

from the Meadowbank gold deposit, Western Churchill Province, Nunavut; Geological Survey of Canada, Current Research 2014-1, 26 p. doi:10.4095/293129

Gourcerol, B., Thurston, P.C., Kontak, D.J., Côté-Mantha, O., and Biczok, J.,2015. Distinguishing primary and mineralization-related signatures of chert from the banded iron formation-type gold deposits at Musselwhite, Ontario and Meadowbank, Nunavut; Geological Survey of Canada, Current Research 2015-1, 21 p.

Grunsky, E.C., Brauhart, C., Hagemann, S., and Dubé, B., 2015. The magmato-hydrothermal space: a new metric for geochemical characterization of ore deposits; Geological Survey of Canada, Open File 7487, 1 sheet. doi:10.4095/295662

Janvier, V., Castonguay, S., Mercier-Langevin, P., Dubé, B., McNicoll, V., Malo, M., Pehrsson, S., and Bécu, V., 2013. Recognizing optimum Banded-Iron Formation-hosted gold environments in ancient, deformed and metamorphosed terranes: Preliminary results from the Meadowbank deposit, Nunavut, Canada; Geological Survey of Canada, Open File 7407, 1 sheet. doi:10.4095/292589

Janvier, V., Castonguay, S., Mercier-Langevin, P., Dubé, B., McNicoll, V., Pehrsson, S., Malo, M., De Chavigny, B., and Côté-Mantha, O., 2015. Preliminary results of the geology of the Portage deposit, Meadowbank gold mine, Churchill Province, Nunavut; Geological Survey of Canada, Current Research 2015-2, 21 p. doi:10.4095/295532

Kelly, C.J., Gagnon, É, and Schneider, D.A., 2013. Redefining the pattern and timing of metamorphism in the North Caribou greenstone belt. Ontario Geological Survey, *In:* Summary of Field Work and other Activities 2013; Ontario Geological Survey, Open File Report 6290, p. 59-1 to 59-8.

Lafrance, B., Tóth, Z., Dubé, B., and Mercier-Langevin, P., 2012. Geological setting of banded iron formation-hosted gold mineralization in the Geraldton area, Northern Ontario, *In:* Summary of Field Work and other Activities 2012; Ontario Geological Survey, Open File Report 6280, p. 48-1 to 48-10.

Lawley, C.J.M., Creaser, R.A., McNicoll, V., Dubé, B., Mercier-Langevin, P., Pehrsson, S., and Vaillancourt, D., 2014. Re-Os arsenopyrite and U-Pb detrital zircon geochronology at the Meliadine Gold District, Nunavut: implications for the geologic setting and age of the Tiriganiaq Deposit; Geological Survey of Canada, Open File 7510, 19 p. doi:10.4095/293939

Lawley, C.J.M., Dubé, B., Jackson, S., Yang, Z., and Mercier-Langevin, P., 2014. Sulfide paragenesis and LA-ICP-MS arsenopyrite geochemistry at the Meliadine Gold District, Nunavut: implications for Re-Os arsenopyrite geochronology and ore deposit genesis; Geological Survey of Canada, Open File 7491, 1 sheet. doi:10.4095/293938

Lawley, C.J.M., Creaser, R.A., Jackson, S., Yang, Z., Davis, B., Dubé, B., Mercier-Langevin, P., Pehrsson, S., and Vaillancourt, D., 2015. Protracted Paleoproterozoic gold history at the Archean BIF-hosted Meliadine Gold District, Nunavut; Geological Survey of Canada, Open File 7743, 23 p. doi:10.4095/295629

Lawley, C.J.M., Dubé, B., Mercier-Langevin, P., Kjarsgaard, B.A., and Knight, R.D., 2015. Whole-rock lithogeochemistry and pXRF data from the Meliadine gold district, Nunavut, Canada; Geological Survey of Canada, Open File 7711, 1 .zip file. doi:10.4095/296223

Lawley, C.J.M., Dubé, B., Mercier-Langevin, P., and Vaillancourt, D., 2015. Mapping hydrothermal footprints: case studies from the Meliadine Gold District, Nunavut; Geological Survey of Canada, Open File 7744, 22 p. doi:10.4095/295920

Mercier-Langevin, P., Goutier, J., Ross, P.-S., McNicoll, V., Monecke, T., Dion, C., Dubé, B., Thurston, P., Bécu, V., Gibson, H., Hannington, M., and Galley, A., 2011. The Blake River Group of the Abitibi greenstone belt and its unique VMS and gold-rich VMS endowment, GAC-MAC-SEG-SGA Annual Meeting, Ottawa, Ontario, May 2011, Field Trip 02B guidebook; Geological Survey of Canada, Open File 6869, 61 p.

Oswald, W., Dubé, B., Castonguay, S., McNicoll, V., Biczok, J., Mercier-Langevin, P., Malo, M., and Skulski, T., 2014. New insights on the structural and geological setting of the world-class Musselwhite gold deposit, Superior Province, Northwestern Ontario; Geological Survey of Canada, Open File 7633, 1 sheet. doi:10.4095/294817

Oswald, W, Castonguay, S., Dubé, B., Mercier-Langevin, P., Malo, M., Biczok, J., and McNicoll, V., 2014. Targeted Geoscience Initiative 4. Lode gold deposits in ancient deformed and metamorphosed terranes: detailed mapping of key stripped outcrops in the Musselwhite Mine area, Northwestern Ontario, and implications for the geological and structural setting of the gold mineralization, *In:* Summary of Field Work and Other Activities 2014; Ontario Geological Survey, Open File Report 6300, p. 42-1 to 42-15.

Oswald, W., Castonguay, S., Dubé, B., McNicoll, V., Biczok, J., Malo, M., and Mercier-Langevin, P., in press. New insights on the geological and structural settings of the Musselwhite banded iron formation-hosted gold deposit, North Caribou greenstone belt, Superior Province, Ontario; Geological Survey of Canada, Current Research 2015-3, 19 p.

Pelletier, M., Mercier-Langevin, P., Crick, D., Tolman, J., Beakhouse, G.P., and Dubé, B., 2014. Preliminary observations on the nature and distribution of the deformed and metamorphosed hydrothermal alteration associated with the Archean Rainy River gold deposit, northwestern Ontario; Ontario Geological Survey, Open File Report 6300, p. 41-1 to 41-10.

Tóth, Z., Lafrance, B., Dubé, B., Mercier-Langevin, P., and McNicoll, V, 2013. Geological setting of banded iron formation-hosted gold mineralization in the Geraldton area, Northern Ontario: preliminary results; Geological Survey of Canada, Open File 7370, 54 p. doi:10.4095/292558

Tóth, Z., Lafrance, B., Dubé, B., Mercier-Langevin, P., and McNicoll, V., 2013. Targeted Geoscience Initiative 4. Lode gold deposits in ancient deformed and metamorphosed terranes: geological mapping and structural reappraisal of the banded iron formation-hosted gold mineralization in the Geraldton area, Ontario, *In:* Summary of Field Work and other Activities 2013; Ontario Geological Survey, Open File Report 6290, p. 58-1 to 58-14.

Tóth, Z., Lafrance, B., Dubé, B., Mercier-Langevin, P., and McNicoll, V.J., 2014. Targeted Geoscience Initiative 4. Lode gold deposits in ancient deformed and metamorphosed terranes: relative chronology between hydrothermal activity, gold mineralization and deformation events in the Geraldton area, NW Ontario, *In:* Summary of Field Work and Other Activities 2014; Ontario Geological Survey, Open File Report 6300, p. 40-1 to 40-10.

Wright-Holfeld, A., Mercier-Langevin, P., and Dubé, B., 2011. Mass changes and element mobility associated with the Westwood deposit ore zones, Doyon-Bousquet-LaRonde mining camp, Abitibi, Quebec; Geological Survey of Canada, Current Research 2011-8, 19 p. doi:10.4095/288023

Yergeau, D., Mercier-Langevin, P., Dubé, B., Jackson, S., Malo, M., Bernier, C., and Simard, P., 2014. Synvolcanic Au-Cu±Ag-Zn-Pb massive sulphides, veins and disseminations of the Westwood deposit, Abitibi greenstone belt, Québec; Geological Survey of Canada, Open File 7482, 54 p. doi:10.4095/293117

STUDENT THESES

Beauchamp A.-M., en préparation. Géologie, styles de minéralisation et d'altération de l'indice aurifère Mustang, Ceinture de roches vertes de la Basse-Eastmain, Province du Supérieur, Québec; Mémoire de maîtrise (M.Sc.), Institut national de la recherche scientifique – Centre Eau Terre Environnement, Québec, Québec.

Fontaine, A., en préparation. Géologie et genèse de la mine Éléonore, gisement aurifère Roberto, Baie James, Province du Supérieur, Québec, Canada; Thèse de doctorat (Ph.D.), Institut national de la recherche scientifique – Centre Eau Terre Environnement, Québec, Québec.

Goucerol, B., in preparation. Banded-Iron Formation primary geochemistry signatures, and exploration implications for BIF-hosted Au deposits; Ph.D. thesis, Laurentian University, Sudbury, Ontario.

Janvier, V., en préparation. Géologie et caractéristiques structurales du gisement aurifère Meadowbank, Nunavut, Canada; Thèse de doctorat (Ph.D.), Institut national de la recherche scientifique – Centre Eau Terre Environnement, Québec, Québec.

Katz, L., in preparation. The geology, alteration and mineralization of the Archean intrusion-related Côté Gold Au(-Cu) deposit; Ph.D. thesis, Laurentian University, Sudbury, Ontario.

Kelly, C.J., in prep. Dating the metamorphic veil of the North Caribou Superterrane via SIMS depth-profiling; Ph.D. thesis, University of Ottawa, Ottawa, Ontario.

Oswald, W., in prep. Structural and geological setting of the world-class Musselwhite gold deposit, Superior Province, Northwestern Ontario; Ph.D. thesis, Institut national de la recherche scientifique – Centre Eau Terre Environnement, Québec, Québec.

Pelletier, M., in prep. Geologic and structural controls on ore style and distribution in the Archean Rainy River Gold deposit, Wabigoon Subprovince, Ontario; M.Sc. thesis, Institut national de la recherche scientifique – Centre Eau Terre Environnement, Québec, Québec.

Ravenelle, J.-F., 2013. Amphibolite-facies gold mineralization: an example from the Roberto deposit, Eleonore property, James Bay, Quebec; Ph.D thesis, Institut national de la recherche scientifique – Centre Eau Terre Environnement, Québec, Québec, 283 p.

Tóth, Z., in prep. Banded iron formation-hosted gold mineralization – Beardmore-Geraldton area: structural setting, footprint(s), and exploration implications; Ph.D. thesis, Laurentian University, Sudbury, Ontario.

Yergeau, D., 2015. Géologie du gisement synvolcanique aurifère atypique Westwood, Abitibi, Québec; thèse de doctorat (Ph.D.), Institut national de la recherche scientifique – Centre Eau Terre Environnement, Québec, Quebec, 682 p.

CONFERENCE PROCEEDINGS/ABSTRACTS

Beauchamp, A.-M., Dubé, B., Malo, M., Archer, P., Chartrand, F., and Lavoie, J., 2014. Geology of the turbidite-hosted Mustang gold showing, lower Eastmain greenstone belt, Superior Province, Quebec, *In:* Program with Abstracts; Geological Association of Canada – Mineralogical Association of Canada Annual Joint Meeting, Fredericton, New Brunswick, May 2014, v. 37, p. 22.

Beauchamp, A.M., Dubé, B., Malo, M., Archer, P., Chartrand, F., and Lavoie, J., 2014. Geology of the turbidite-hosted Mustang gold showing, lower Eastmain greenstone belt, Superior Province, Quebec: preliminary results, *In:* Abstracts; Prospectors and Developers Association of Canada – Society of Economic Geologists Student Minerals Colloquium, Prospectors and Developers Association of Canada International Trade Show and Investors Exchange, Toronto, Ontario, March 3rd, 2014. Available on-line at https://cmic-footprints.ca/pdac-smc/2014

Beauchamp, A.-M., Dubé, B., Malo, M., Archer, P., Lavoie, J. et Chartrand, F., 2015. Géologie, styles de minéralisation et d'altération de l'indice aurifère Mustang, Ceinture de roches vertes de la Basse-Eastmain, Province du Supérieur, Québec, Dans: Résumés des conférences et des photoprésentations; Québec Mines 2014, Ministère de l'Énergie et des Ressources naturelles du Québec, Québec, novembre 2014, DV 2015-03, p. 67.

Beaudoin, G., Mercier-Langevin P., Dubé, B., and Taylor, B.E., 2011. Low-temperature hydrothermal alteration at the world-class gold-rich VMS LaRonde Penna mine, Abitibi, Québec: An oxygen isotope study, *In:* Program with Abstracts; Geological Association of Canada – Mineralogical Association – Society of Economic Geologists – Society for Geology Applied to Mineral Deposits Annual Joint Meeting, Ottawa, Ontario, May 2011, v. 34, p. 13.

Bleeker, W., 2013. Major faults, synorogenic clastic deposits, and gold mineralization in Archean cratons: syn-orogenic extension followed by thick-skinned thrust burial, and final strike-slip, *In:* Program with Abstracts; Geological Association of Canada – Mineralogical Association of Canada Annual Joint Meeting, Winnipeg, Manitoba, May 2013, v. 36, p. 70–71.

Bleeker, W., 2014. The Abitibi breaks: Syn-orogenic extensional faults inverted as thick-skinned thrusts, and explaining the link with economic gold mineralization, Canada, *In:* Program with Abstracts; Geological Association of Canada – Mineralogical Association of Canada Annual Joint Meeting Fredericton, New Brunswick, May 2014, v. 37, p. 32–33.

Boudreau, C., Mercier-Langevin, P. Goutier, J. et Dubé, B., 2013. Caractérisation des unités volcaniques felsiques et des brèches de coulée à fragments de sulfures de la partie supérieure de la Formation de Rouyn-Pelletier, Rouyn-Noranda, Québec, Dans: Résumés des conférences et des photoprésentations; Québec Mines 2012, Ministère des Ressources naturelles du Québec, Quebec, novembre 2012, DV 2013-03, p. 51.

Castonguay, S., Janvier, V., Mercier-Langevin, P., Dubé, B., McNicoll, V., Malo, M., Pehrsson, S. and Bécu, V., 2012. Recognizing optimum Banded-Iron Formation-hosted gold environments in ancient, deformed and metamorphosed terranes: Preliminary results from the Meadowbank deposit, Nunavut, *In:* YKGSF Abstracts Volume, (comp.) D.M. Watson; 40th Annual Yellowknife Geoscience Forum, Northwest Territories Geoscience Office, Yellowknife, NWT, November 2012, v. 2012, p. 54.

De Souza, S., Dubé, B., McNicoll, V., Mercier-Langevin, P., de Chavigny, P., Gervais, D. et Caron, L., 2013. La mine Canadian Malartic, Abitibi: Observations préliminaires des caractéristiques géologiques et de la chronologie relative des minéralisations aurifères archéennes à basse teneur et fort tonnage, Dans: Résumés des conférences et des photoprésentations; Québec Mines 2012, Ministère des Ressources naturelles du Québec, Québec, novembre 2012, DV 2013-03, p. 45.

De Souza, S., Dubé, B., McNicoll, V., Mercier-Langevin, P., Dupuis, C., Creaser, R., de Chavigny, P. and Gervais, D., 2014. La mine Canadian Malartic, Abitibi, Québec: caractéristiques géologiques et chronologie relative de la minéralisation aurifères à basse teneur et fort tonnage, Dans: Résumés des conférences et des photoprésentations; Québec Mines 2013, Ministère des Ressources naturelles du Québec, Québec, novembre 2013, DV 2014-03, p. 16.

De Souza, S., Dubé, B., McNicoll, V., Dupuis, C., Mercier-Langevin, P. and Creaser, R., 2014. The Canadian Malartic world-class gold deposit: toward a multiphase model for Archean sediment- and porphyry-hosted low-grade large tonnage gold deposit, *In:* Abstracts; Prospectors and Developers Association of Canada – Society of Economic Geologists Student Minerals Colloquium, Prospectors and Developers Association of Canada International Trade Show and Investors Exchange, Toronto, Ontario, March 3rd, 2014. Available on-line at https://cmic-footprints.ca/pdac-smc/2014

De Souza, S., Dubé, B., McNicoll, V., Dupuis, C., Mercier-Langevin,P., and Creaser, R., 2014. Fracture-controlled hydrothermal alteration at the Canadian Malartic deposit: Toward a multiphase model for Archean intrusion-related low-grade bulk tonnage gold deposits, *In:* Program with Abstracts; Geological Association of Canada – Mineralogical Association of Canada Annual Joint Meeting, Fredericton, New Brunswick, May 2014, v. 37, p. 70.

De Souza, S., Dubé, B., Dupuis, C., Mercier-Langevin,P., McNicoll, V. et Creaser, R., 2015. Altération hydrothermale à la mine Canadian Malartic: distribution, minéralogie et géochimie d'un système aurifère archéen complexe et multiphasé, Dans: Résumés des conférences et des photoprésentations; Québec Mines 2014, Ministère de l'Énergie et des Ressources naturelles du Québec, Québec, novembre 2014, DV 2015-03, p. 45.

Dubé, B., Ravenelle, J.F., McNicoll, V., Malo, M., Nadeau, L., Creaser, R.A., and Simoneau, J., 2011. The world-class Roberto gold deposit, Éléonore property, James Bay area, Superior province, Quebec: Insights from geology and geochronology, *In:* Program with Abstracts; Geological Association of Canada – Mineralogical Association – Society of Economic Geologists – Society for Geology Applied to Mineral Deposits Annual Joint Meeting, Ottawa, Ontario, May 2011, v. 34, p. 55–56.

Dubé, B., Ravenelle, J.F., McNicoll, V., Malo, M., Nadeau, L., Creaser, R.A., and Simoneau, J., 2011. The world-class Roberto gold deposit, Éléonore property, James Bay area, Superior province, Quebec: Insights from geology and geochronology, *In:* Program with Abstracts; Geological Association of Canada –

Mineralogical Association – Society of Economic Geologists – Society for Geology Applied to Mineral Deposits Annual Joint Meeting, Ottawa, Ontario, May 2011, v. 34, p. 55–56.

Dupuis, C., Mercier-Langevin, P., McNicoll, V., Janvier, V., Dubé, B., Castonguay, S., de Chavigny, B., Pehrsson, S., and Côté-Mantha, O., 2014. The Vault gold deposit, Meadowbank area, Nunavut: Preliminary results on the nature and timing of mineralization, Canada, *In:* Program with Abstracts; Geological Association of Canada – Mineralogical Association of Canada Annual Joint Meeting, Fredericton, New Brunswick, May 2014, v. 37, p. 81.

Fontaine, A., Dubé B., Malo, M., McNicoll, V., and Brisson, T., 2014. Roberto gold deposit, Eleonore project, Superior Province, James Bay, Quebec, diversity of styles related to structural-metamorphic settings, *In:* Program with Abstracts; Geological Association of Canada – Mineralogical Association of Canada Annual Joint Meeting, Fredericton, New Brunswick, May 2014, v. 37, p. 93–94.

Fontaine, A., Dubé, B., Malo, M., McNicoll, V., and Brisson, T., 2014. Roberto gold deposit, Eleonore project Superior Province, James Bay, Quebec: relationships between tectono-metamorphic settings and ore bodies diversity, *In:* Abstracts; Prospectors and Developers Association of Canada – Society of Economic Geologists Student Minerals Colloquium, Prospectors and Developers Association of Canada International Trade Show and Investors Exchange, Toronto, Ontario, March 3rd, 2014. Available on-line at https://cmic-footprints.ca/pdac-smc/2014

Fontaine, A., Dubé, B., Malo, M., McNicoll, V. et Brisson, T., 2015. Géologie et caractéristiques structurales du gisement aurifère Roberto, propriété Éléonore, Province du Supérieur, Baie-James, Québec, Canada, Dans: Résumés des conférences et des photoprésentations; Québec Mines 2014, Ministère de l'Énergie et des Ressources naturelles du Québec, Québec, novembre 2014, DV 2015-03, p. 68.

Gagnon, E., Schneider, D.A., Hattori, K., and Biczok, J., 2013. Regional Metamorphism and Deformation of the North Caribou Belt (W. Superior Province) and the Relationship with the Lode Gold Mineralization at Musselwhite Mine, *In:* Abstracts; Society of Economic Geologists Annual Meeting, Whistler, British-Columbia, September 2013. Available on-line at http://www.segweb.org/SEG/Events/SEG_Conference_Website_Archives/SEG/_Events/SEG_Conference_Website_Archives

Gao, J.-F., Jackson S.E., and Dubé, B., 2013. Multi-stage gold mineralization at the Hollinger-McIntyre deposit: A LA-ICPMS mapping study, *In:* Goldschmidt 2013 conference abstracts; Mineralogical Magazine, v. 77, p. 1139.

Gao, J.-F., Jackson, S.E., Dubé, B., and De Souza, S., 2014. Gold mineralization in the Canadian Malartic deposit, Canada: Insights from textural and quantitative elemental mapping of pyrite, *In:* Program with Abstracts; Geological Association of Canada – Mineralogical Association of Canada Annual Joint Meeting, Fredericton, New Brunswick, May 2014, v. 37, p. 97–98.

Gourcerol, B., Thurston, P.C., Konak, D.J., and Côté-Mantha, O., 2014. The geochemistry of banded iron formation (BIFs) at the Meadowbank gold deposit, Churchill Province: Implications for the origin of gold mineralization in BIF deposits, *In:* Program with Abstracts; Geological Association of Canada – Mineralogical Association of Canada Annual Joint Meeting, Fredericton, New Brunswick, May 2014, v. 37, p. 107-108.

Gourcerol, B., Thurston, P.C., Kontak, D.J., and Côté-Mantha, O., 2014. The geochemistry of banded iron formation (BIFs) at the Meadowbank gold deposit, Churchill Province: implications for the sources of fluids in gold-mineralized in BIF deposits, *In:* Abstracts; Prospectors and Developers Association of Canada – Society of Economic Geologists Student Minerals Colloquium, Prospectors and Developers Association of Canada International Trade Show and Investors Exchange, Toronto, Ontario, March 3rd, 2014. Available on-line at https://cmic-footprints.ca/pdac-smc/2014

Gourcerol, B., Thurston, P.C., Kontak, D.J., Côté-Mantha, O., and Biczok, J., 2015. Depositional setting of Algoma-type Banded Iron Formation from the Meadowbank, Meliadine and Musselwhite gold deposits, *In:* Abstracts; Prospectors and Developers Association of Canada – Society of Economic Geologists Student Minerals Colloquium, Prospectors and Developers Association of Canada International Trade Show and Investors Exchange, Toronto, Ontario, March 2nd, 2015. Available on-line at http://cmic-footprints.ca/pdac-smc/2015

Jackson, S., Dubé, B., Chapman, J., and Gao, J.-F., 2013. Applications of LA-ICP-MS element mapping in mineral deposit research and exploration, *In:* Proceedings; 12th Biennial Society for Geology Applied to Mineral Deposits Meeting, Uppsala, Sweden, August 2013, v.1, p. 201–204.

Jackson, S., Gao, J. et Dubé, B., 2014. Nouveaux développements applicables à l'analyse des éléments en traces dans les dépôts de minéraux et cartographie utilisée pour la recherche et l'exploration des gisements de minerai: exemples de gisements d'or du Québec et de l'Ontario, Dans: Résumés des conférences et des photoprésentations; Québec Mines 2013, Ministère des Ressources naturelles du Québec, Québec, novembre 2013, DV 2014-03, p. 16.

Janvier, V., Castonguay, S., Mercier-Langevin, P., Dubé, B., Malo, M., McNicoll, V., Pehrsson, S., De Chavigny, B., and Côté-Mantha, O., 2014, Geology of the banded iron formation-hosted Meadowbank gold deposit, Nunavut, Canada, *In:* Program with Abstracts; Geological Association of Canada – Mineralogical Association of

Canada Annual Joint Meeting, Fredericton, New Brunswick, May 2014, v. 37, p. 127.

Janvier, V., Mercier-Langevin, P., Castonguay, S., Dubé, B., McNicoll, V., Pehrsson, S., Malo, M., de Chavigny, B., and Côté-Mantha, O., 2014. Geology and structural relationships of the Meadowbank BIF-hosted gold deposit, Nunavut, Canada, *In:* Abstracts; Prospectors and Developers Association of Canada – Society of Economic Geologists Student Minerals Colloquium, Prospectors and Developers Association of Canada International Trade Show and Investors Exchange, Toronto, Ontario, March 3rd, 2014. Available on-line at https://cmic-footprints.ca/pdac-smc/2014

Katz, L., Kontak, D.J., Dubé, B., McNicoll, V., Creaser, R., and Hamilton, M., 2013. The Archean Coté Gold deposit, Ontario, Canada: A large tonnage, low-grade deposit centred on a 2740 Ma magmatic-hydrothermal diorite breccia complex; *In:* Abstracts; Society of Economic Geologists Annual Meeting, Whistler, British-Columbia, September 2013. Available on-line at http://www.segweb.org/SEG/Events/SEG_Conference_Website_Archives/SEG/_Events/SEG_Conference_Website_Archives

Katz, L.R., Kontak, D.J., and Dubé, B., 2014. Chemical fingerprinting of the Archean Côté Gold deposit: A large-tonnage, low-grade intrusion-related deposit system, Ontario, Canada, *In:* Program with Abstracts; Geological Association of Canada – Mineralogical Association of Canada Annual Joint Meeting, Fredericton, New Brunswick, May 2014, v. 37, p. 134–135.

Katz, L.R., Kontak, D.J., and Dubé, B., 2014. The Archean Côté Gold intrusion-related Au (-Cu) deposit, Ontario, Canada: A largetonnage, low-grade deposit centred on a magmatic-hydrothermal breccia, *In:* Program with Abstracts; Geological Association of Canada – Mineralogical Association of Canada Annual Joint Meeting, Fredericton, New Brunswick, May 2014, v. 37, p. 133-134.

Katz, L.R., Kontak, D.J., Dubé, B., Rogers, J.R., McNicoll, V, and Creaser, R.A., 2014. The Côté Gold Au(-Cu) deposit, Ontario, Canada: an Archean large-tonnage, low-grade deposit centered on a magmatic-hydrothermal breccia, *In:* Abstracts; Prospectors and Developers Association of Canada – Society of Economic Geologists Student Minerals Colloquium, Prospectors and Developers Association of Canada International Trade Show and Investors Exchange, Toronto, Ontario, March 3rd, 2014. Available on-line at https://cmic-footprints.ca/pdac-smc/2014

Kelly, C., Schneider, D., Hattori, K., Biczok, J., and Schmitt, A., 2013. Resolving the Timing of Fluid Flow within Metamorphosed Terranes: U-Pb Age Depth-Profiles of Zircon from the North Caribou Greenstone Belt, Canada, *In:* Abstracts; Society of Economic Geologists Annual Meeting, Whistler, British-Columbia, September 2013. Available on-line at http://www.segweb.org/SEG/Events/SEG_Conference_Website_Archives/SEG/_Events/SEG_Conference_Website_Archives

Kontak, D.J., Katz, L., Creaser, R., and Hamilton, M., 2013. The Archean Côté Gold Au(-Cu) deposit of northern Ontario, Canada : A large tonnage, low-grade Au deposit centred on a 2740 Ma magmatic-hydrothermal diorite complex, *In:* Program with Abstracts; Geological Association of Canada – Mineralogical Association of Canada Annual Joint Meeting, Winnipeg, Manitoba, May 2013, v. 36, p. 122–123.

Lawley, C.J.M., Dube, B., Jackson, S., and Mercier-Langevin, P., 2013. Sulfide paragenesis and LA-ICP-MS arsenopyrite geochemistry at the Meliadine Gold District, Nunavut: Implications for Re-Os arsenopyrite geochronology and ore deposit genesis, *In:* Abstracts; Society of Economic Geologists Annual Meeting, Whistler, British-Columbia, September 2013. Available on-line at http://www.segweb.org/SEG/Events/SEG_Conference_Website_Archives/SEG/_Events/SEG_Conference_Website_Archives SEG-Whistler2013

McNicoll, V., Dubé, B., Biczok, J., Castonguay, S., Oswal, W., Mercier-Langevin, P., Skulski, T., and Malo, M., 2013. The Musselwhite gold deposit, North Caribou greenstone belt, Ontario: new high precision U-Pb ages and their impact on the geological and structural setting of the deposit, *In:* Program with Abstracts; Geological Association of Canada – Mineralogical Association of Canada Annual Joint Meeting, Winnipeg, Manitoba, May 2013, v. 36, p. 142.

Mercier-Langevin, P., Dubé, B., Yergeau, D., Galley, A., Wright-Holfeld, A., and Hannington, M., 2011. The Archean Westwood gold deposit, Abitibi: contrasting styles of auriferous mineralization and hydrothermal alteration, *In:* Program with Abstracts; Geological Association of Canada – Mineralogical Association of Canada – Society of Economic Geologists – Society for Geology Applied to Mineral Deposits Annual Joint Meeting, Ottawa, Ontario, May 2011, v. 34, p. 140.

Mercier-Langevin, P., Hannington, M., Dubé, B., and Bécu, V. 2011. The gold content of volcanogenic massive sulphide deposits, *In:* Conference Guide; Conference of Metallurgists 2011, World Gold 2011 meeting, Montreal, October 2011, p. 47–48.

Mercier-Langevin, P., Hannington, M., Dubé, B., McNicoll, V., Goutier, J., and Monecke, T., 2011. Geodynamic influences on the genesis of Archean world-class gold-rich VMS deposits: examples from the Blake River Group, Abitibi greenstone belt, Canada, *In:* Proceedings; 11th Biennal Society for Geology Applied to Mineral Deposits Meeting, Antofagasta, Chile, September 2011, p. 85–87.

Mercier-Langevin, P., Hannington, M., Dubé, B., McNicoll, V., Goutier, J., and Monecke, T., 2013. Geodynamic influences on the genesis of Archean world-class gold-rich VMS deposits: examples from the Blake River Group, Abitibi greenstone belt, Canada, *In:* Program with Abstracts; Geological Association of Canada-

Mineralogical Association of Canada Annual Joint Meeting, Winnipeg, Manitoba, May 2013, v. 36, p. 144–145.

Mercier-Langevin, P., Dubé, B., Hannington, M., and Bécu, V., 2012. The gold content of VMS deposits: Key features and controlling parameters, with implications for exploration in the Appalachain orogen, *In:* Program with Abstracts; Geological Association of Canada – Mineralogical Association of Canada Annual Joint Meeting, St-John's, Newfoundland, May 2012, v. 35, p. 91.

Mercier-Langevin, P., Lafrance, B., Bécu, V., Dubé, B., Kjarsgaard, I., Guha, J., and Ross, P.-S., 2013. Geology, alteration and mineralization of the Lemoine auriferous VMS deposit, Chibougamau camp, Abitibi greenstone belt, Quebec: Geologic evidence for a magmatic input, *In:* Program with Abstracts; Geological Association of Canada – Mineralogical Association of Canada Annual Joint Meeting, Winnipeg, Manitoba, May 2013, v. 36, p. 145.

Oswald, W., Dubé, B., Castonguay, S., McNicoll, V., Biczok, J., Mercier-Langevin, P., Malo, M., and Skulski, T., 2014. New insights on the geological setting of the world-class Musselwhite gold deposit, Superior Province, northwestern Ontario, *In:* Program with Abstracts; Geological Association of Canada – Mineralogical Association of Canada Annual Joint Meeting, Fredericton, New Brunswick, May 2014, v. 37, p. 311.

Oswald, W., Dubé, B., Castonguay, S., McNicoll, V., Biczok, J., Mercier-Langevin, P., Malo, M., and Skulski, T., 2014. New insights on the structural and geological setting of the world-class Musselwhite gold deposit, Superior Procvince, Northwestern Ontario, *In:* Abstracts; PDAC-SEG Student Minerals Colloquium, Prospectors and Developers Association of Canada International Trade Show and Investors Exchange, Toronto, Ontario, March 3rd, 2014. Available on-line at https://cmic-footprints.ca/pdac-smc/2014

Pelletier, M., Mercier-Langevin, P., Tolman, J., McNicoll, V., Dubé, B., Richer-Laflèche, M. and Beakhouse, G., 2014. Geologic and structural controls on ore style and distribution in the Archean Rainy River Gold deposit, Wabigoon Subprovince, Ontario: Preliminary results, *In:* Program with Abstracts; Geological Association of Canada – Mineralogical Association of Canada Annual Joint Meeting, Fredericton, New Brunswick, May 2014, v. 37, p. 218–219.

Pelletier, M., Mercier-Langevin, P., Tolman, J., McNicoll, V., Dubé, B., Richer-Laflèche, M., and Beakhouse, G., 2014. The Rainy River gold project, Wabigoon Subprovince, Ontario: preliminary observations on ore zone's geometry and style, and associated alteration, *In:* Abstracts; PDAC-SEG Student Minerals Colloquium, Prospectors and Developers Association of Canada International Trade Show and Investors Exchange, Toronto, Ontario, March 3rd, 2014. Available on-line at https://cmic-footprints.ca/pdac-smc/2014

Smith, J., Lafrance, B., and Kontak, D., 2014. A comparative study of the deformation history of auriferous quartz veins in the Archean Côté Gold deposit and the structural evolution of the spatially-related Ridout Deformation Zone, Swayze Greenstone Belt, northern Ontario, *In:* Program with Abstracts; Geological Association of Canada – Mineralogical Association of Canada Annual Joint Meeting, Fredericton, New Brunswick, May 2014, v. 37, p. 257–258.

Tóth, Z., Lafrance, B., Dubé, B., McNicoll, V.J., and Mercier-Langevin, P., 2014. Stratigraphic and structural setting of banded-iron-formation-hosted gold mineralisation in the Geraldton area, Ontario, *In:* Program with Abstracts; Geological Association of Canada – Mineralogical Association of Canada Annual Joint Meeting, Fredericton, New Brunswick, May 2014, v. 37, p. 272–273.

Tòth, Z., Lafrance, B., Dubé, B., Mercier-Langevin, P., and McNicoll. V., 2014. Structural setting, mineralogical characteristics and geochemical footprints of banded-iron-formation-hosted gold mineralisation in the Geraldton area, Ontario, *In:* Abstracts; Prospectors and Developers Association of Canada – Society of Economic Geologists Student Minerals Colloquium, Prospectors and Developers Association of Canada International Trade Show and Investors Exchange, Toronto, Ontario, March 3rd, 2014. Available on-line at https://cmic-footprints.ca/pdac-smc/2014

Yergeau, D., Mercier-Langevin, P., Malo, M., Dubé, B., Bernier, C., Savoie, A., Houle, N., et Simard, P., 2011. Géologie de la lentille de sulfures massifs polymétalliques aurifères Warrenmac, gisement Westwood, Abitibi, Québec, Dans: Résumés des conférences et des photoprésentations; Québec Exploration 2011, Ministère des Ressources naturelles et de la Faune du Québec, Québec, novembre 2011, DV 2011-03, p. 39.

Yergeau, D., Mercier-Langevin, P., et al., 2012. The Westwood deposit, southern Abitibi greenstone belt: a "hybrid" or "transitional" Archean gold deposit, *In:* Program with Abstracts; Geological Association of Canada – Mineralogical Association of Canada Annual Joint Meeting, Newfoundland, May 2012, v. 35, p. 154.

Yergeau, D., Mercier-Langevin, P., Dubé, B., Malo, M., Bernier, C., Savoie, A., and Simard, P., 2013. Synvolcanic Au-Cu±Ag-Zn-Pb massive sulphides, veins and disseminations of the Westwood deposit, Abitibi greenstone belt, Québec, *In:* Program with Abstracts; Geological Association of Canada – Mineralogical Association of Canada Annual Joint Meeting, Winnipeg, Manitoba, May 2013, v. 36, p. 201.

Yergeau, D., Mercier-Langevin, P., Dubé, B., Malo, M., Goutier, J. Bernier, C., Savoie, A., Houle, N. et Simard, P., 2013. Le gisement Westwood Abitibi, Québec: un sytème magmatique-hydrothermal aurifère archéen?, Dans: Résumés des conférences et des photoprésentations; Québec Mines 2012, Ministère des Ressources naturelles du Québec, Québec, novembre 2012, DV 2013-03, p. 51.